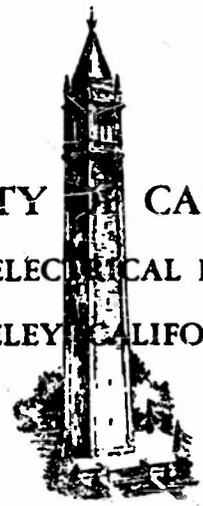

UNIVERSITY OF CALIFORNIA

DIVISION OF ELECTRICAL ENGINEERING

BERKELEY, CALIFORNIA

ELECTRONICS RESEARCH LABORATORY

PROPERTIES OF LARGE SLOT ANTENNAS

by

A. E. Ratkevich

Institute of Engineering Research

Series No. 60, Issue No. 104

December 1, 1953

DIVISION OF ELECTRICAL ENGINEERING
ELECTRONICS RESEARCH LABORATORY

SERIES NO. 60
ISSUE NO. 104

ANTENNA GROUP

Report No. 22 on
Office of Naval Research
Contract N7onr-29529

PROPERTIES OF LARGE SLOT ANTENNAS

Prepared by: A. E. Ratkevich

A. E. Ratkevich, Junior Research Engineer

Edited by: Samuel Silver

Samuel Silver, Professor of Engineering Science

Approved by: J. R. Whinnery

J. R. Whinnery, Vice-Chairman, Division of Electrical Engineering, in charge of Electronics Research Laboratory

ABSTRACT

An experimental investigation is made of the field configuration existing in aperture radiators of rectangular shape cut in the broad side of a standard 1" by 0.5" X-band waveguide. All apertures have one dimension equal to a half free space wavelength; the other dimension varies from a half wavelength to two wavelengths. Both far zone measurements and probe measurements in the aperture are limited to amplitude readings. An attempt is made to correlate the distribution in the neighborhood of the aperture determined by means of a probe with the aperture field configuration obtained from synthesis of the far zone patterns. Two different hypotheses are assumed:

(1) In accordance with what has been established for apertures whose lengths, in terms of wavelength, are very large, each component of the electric field distribution in the aperture may be described by a single traveling wave mode (plus a reflected wave) characterized by a complex propagation constant.

(2) The slot field distribution may be described in terms of a finite number of standing wave modes.

The standing wave mode hypothesis is shown to be the most reliable. Best results are obtained for the tangential component of the electric vector which is transverse to the long axis of the aperture. Spurious radiation at the edges, with polarization parallel to the long axis of the aperture introduces errors which make correlation between the measured longitudinal component and the simple theoretical mode configurations very poor.

CONTENTS

ILLUSTRATIONS

I. Introduction

An aperture in the wall of a waveguide which perturbs the current distribution existing over the wall of the guide for a given waveguide mode effects electromagnetic coupling between the interior and the outside and serves as a radiating element for that waveguide mode. Slots are a special case of aperture radiators whose length is large compared to the width. The properties of slot radiators whose lengths are comparable with the wavelength or very much greater than the wavelength have been investigated in considerable detail and such elements have found widespread applications. Reviews of the extensive work done in this field during the war are given in the books by Watson[1] and Silver[2].

The radiation characteristics of the aperture are determined by the field configuration in the aperture itself. In the case of slots this configuration is relatively simple. The electromagnetic Babinet principle[3] has proved to be very useful in this connection and the properties of slots have been well coordinated with those of wire antennas. A wider variety of field configurations can be generated in rectangular apertures whose width is comparable with the length and correspondingly a wider variety of radiation patterns can be obtained. Such radiating elements may be useful either singly or in combinations to produce required complex beam patterns.

The following discussion pertains to rectangular apertures cut in the broad face of a standard 1" x 0.5" waveguide supporting the TE_{10}-mode. The aperture in each case is symmetrical with respect to the axis of the waveguide as shown in Figure 1 (Section II). The aperture dimension b, transverse to the waveguide axis, is a half free space wavelength in each case. The object of this study is to determine how the excitation in the aperture depends on the dimension a, along the axis of the guide.

The region between the narrow slot ($a \leq \lambda/8$) and the long slot ($a \gg \lambda$) has yet to be investigated. It has been established[4] that the field configuration in the long slot (in the region of about 7 wavelengths and longer) may be described by a single traveling wave mode characterized by a complex propagation constant; assuming the slotted waveguide dimensions limit propagation to a single mode.

The question arises as to just how small the dimension a can be while the aperture yet supports the characteristic traveling wave of the long slot.

In the other extreme of the narrow slot, the aperture field is constant in amplitude and phase in the direction of the waveguide axis. Up to the value $a = \lambda/4$, this constant distribution in the longitudinal direction is still a good approximation. At a value $a = \lambda/2$, the far zone pattern exhibits an asymmetry which indicates a phase variation across the aperture in the longitudinal direction. In addition, the aperture commences to support a transverse polarization. As the dimension a is increased further, patterns for both polarizations take on a constantly increasing directivity.

It has been shown[5] that a good approximation to the far zone pattern of a square aperture, edge length equal to a half-wavelength, can be obtained by assuming the aperture to be supporting two modes of excitation: a constant mode E_o and a half sine mode. If this is a valid hypothesis, it is then to be expected that as a is increased, higher order modes will be supported by the aperture. The increase of phase variation across the aperture with an increasing number of standing wave modes could well account for the increasing pattern directivity.

However, from the traveling wave mode point of view, this increasing directivity can also be accounted for. That the phase constant be a function of the longitudinal dimension is not a satisfactory hypothesis to make. The most likely

explanation is that the increase of pattern directivity with an increase of length is due to the decrease of energy remaining in the traveling wave reflected from the end of the aperture. In other words, for the shorter apertures and where the traveling wave has a low attenuation constant, the positively traveling wave plus the reflected wave add up to give a net field distribution which constitutes a single standing wave type of mode. The small net phase variation clouds the larger phase variation of the positively traveling wave.

Consequently it was considered advisable to attempt to arrive at the slot field configuration by utilizing two different hypotheses:

(1) The slot field distribution for each E field polarization may be described by a single traveling wave mode characterized by a complex propagation constant.

(2) The slot field distribution may be described in terms of a finite number of unattenuated standing wave modes;* the number of modes being dependent to some degree on the dimensions of the slot with respect to free space wavelength.

Probe measurements in apertures of the small dimensions to be investigated may be of questionable value when considered alone. However, when considered in conjunction with the slot field distribution obtained by synthesis of the far zone patterns, the probed distribution can be expected to be of some use despite the large error. As this project is not meant to be an exhaustive study of the problem, measurements in the aperture and in the far zone are limited to amplitude measurements; thus simplifying the experimentation and allowing a greater region of aperture dimensions to be investigated in the time available. Phase

* In general a Fourier representation of the field involves an infinite number of modes; it is assumed that all but a certain finite number make a negligible contribution to the properties of the aperture.

measurements to assure uniqueness will be left to a more extensive study of the excitation of aperture radiators in waveguides.

II. Diffraction Pattern and Aperture Distribution

The system of coordinates relating the aperture field to the far zone field is shown in Figure 1.

Aperture Distribution:

The waveguide is supporting the TE_{01} mode and is assumed to be terminated in its own characteristic impedance. By hypothesis (1), the aperture distribution may be described by a single traveling wave mode of the form:

$$E_x(x,y) = f_1(x)\,g_1(y) = (e^{-\gamma_1 x} + \Gamma_1 e^{-\gamma_1 a}\, e^{+\gamma_1 x}) = \cos\frac{\pi y}{b} \qquad (1)$$

$$E_y(x,y) = f_2(x)\,g_2(y) = (e^{-\gamma_2 x} + \Gamma_2 e^{-\gamma_2 a}\, e^{+\gamma_2 x}) = \sin\frac{\pi y}{b} \qquad (2)$$

where $\gamma = \alpha + j\beta$ $\quad \beta$ = phase constant

α = attenuation constant

Γ = reflection coefficient of the end of the slot

The simplifying assumption is made that the end of the slot behaves as an ideal short circuit to the energy remaining in the traveling wave slot mode; thus:

$$\Gamma_1 = +1, \quad \Gamma_2 = -1$$

Since $f_2(x)$ must be zero at $x = \pm a/2$, equation (2) does not hold for $x = -a/2$. If such a traveling wave distribution does occur, a sudden drop of E_y at x close to $-a/2$ is to be expected. For integration purposes this drop of field intensity is assumed to be infinitely sharp, allowing integration over the full slot length.

The simple type of y dependence assumed for $g_1(y)$ is based on the considerations that it satisfies the boundary conditions at $y = \pm a/2$ and that the aperture is resonant to this mode since the dimension in the y-direction is $\lambda/2$. All higher order sinusoids are expected to have much smaller amplitudes.

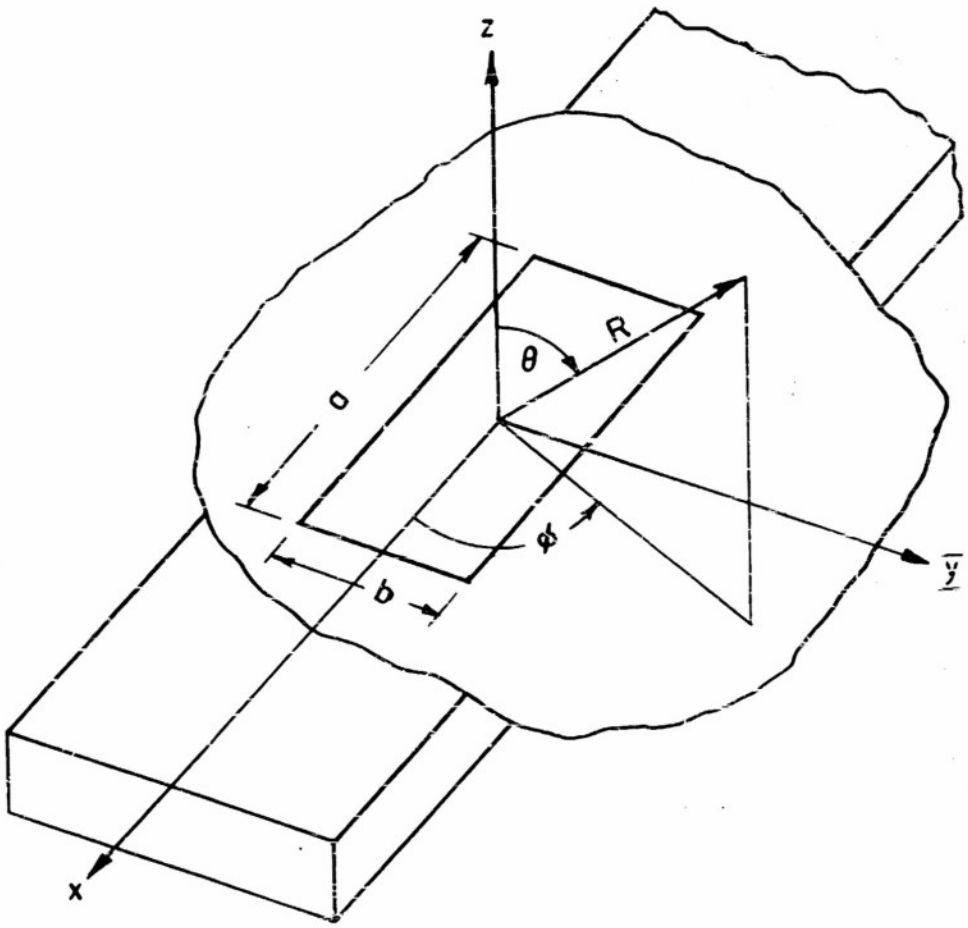

Fig. 1

SPHERICAL COORDINATE SYSTEM AND RECTANGULAR SLOT IN AN INFINITE SHEET IN THE x – y PLANE

WAVEGUIDE SUPPORTS THE TE_{01} MODE PROPAGATING IN THE POSITIVE x DIRECTION

If the slot region is thought of in terms of a short section of waveguide supporting the TE type of mode (E_x, E_y, and H_z), $g_2(y)$ is then obtained by differentiation of $g_1(y)$. Aside from that consideration, the use of an odd function for $g_2(y)$ across the slot is suggested by the nature of the transverse current flow in the unperturbed driving mode in the waveguide which the sides of the slot intercept.

The form of $g_1(y)$ and $g_2(y)$ is verified by the far zone patterns shown in graphs (1) and (2).

By hypothesis (2), the aperture distribution may be described in terms of a finite number of resonant modes of the form:

$$E_y(x,y) = f_2(x)\,g_2(y) = \left(A_m \cos\frac{m\pi x}{a} + B_n \sin\frac{n\pi x}{a}\right)\sin\frac{\pi y}{b} \qquad (3)$$

where, to satisfy the boundary conditions,

m = odd, n = even integer

$$E_x(x,y) = f_1(x)\,g_1(y) = \left(C_n \cos\frac{n\pi x}{a} + D_m \sin\frac{m\pi x}{a}\right)\cos\frac{\pi y}{b}$$

where, by analogy with the solution for a short waveguide of length equal to the slot depth,

n = 0 or even, m = odd integer

A_m, B_n, C_n, D_m, are in general complex constants

The number of dominant modes entering into the representation of the field in the slot is, to be sure, a function of the slot length. For example, a slot length of a full wavelength may be expected to support only modes having a full period or less. As was noted before, the basic idea in the analysis is that all other modes play a secondary part particularly as far as the radiation pattern is concerned.

Diffraction Patterns:

Integration of the vector Helmholtz equations[2] gives the following far

zone fields for the case of an aperture in an infinite ground plane.

In the plane $\phi = 0$

$$E_\theta = \frac{jk}{2\pi R} e^{-jkR} \int_A E_x(x,y)\, e^{jkx \sin\theta}\, dx\, dy \tag{5}$$

$$E_\phi = \frac{jk}{2\pi R} e^{-jkR} \cos\theta \int_A E_y(x,y)\, e^{jkx \sin\theta}\, dx\, dy \tag{6}$$

In the plane $\phi = \pi/2$

$$E_\theta = \frac{jk}{2\pi R} e^{-jkR} \int_A E_y(x,y)\, e^{jky \sin\theta}\, dx dy \tag{7}$$

$$E_\phi = -\frac{jk}{2\pi R} e^{-jkR} \cos\theta \int_A E_x(x,y)\, e^{jky \sin\theta}\, dx dy \tag{8}$$

where k = free space phase constant

Examination of equations (3) and (6) show that since $g_2(y)$ is an odd function, the diffraction pattern for E_ϕ in the plane $\phi = 0$ is always equal to zero. Therefore, another plane is necessary in order to obtain a pattern that is a function of $f_2(x)$ alone.

Figure (2) shows the system of coordinates used as an alternative.

The general expression for the E_y component of the far zone field can be written in the form:

$$E_y = \frac{jk}{2\pi R} e^{-jkR} \sin\alpha \cos\psi \int_A E_y(x,y)\, e^{jk(x \sin\alpha \sin\psi + y \cos\alpha)}\, dx dy \tag{9}$$

For α constant (by keeping ρ and R constant), (9) simplifies to the form:

$$E_y = \frac{jkK}{2\pi R} e^{-jkR} \cos\psi \int_{-\frac{a}{2}}^{+\frac{a}{2}} f_2(x)\, e^{jkx \sin\alpha \sin\psi}\, dx \tag{10}$$

where K is a constant obtained by integrating $g_2(y)$.

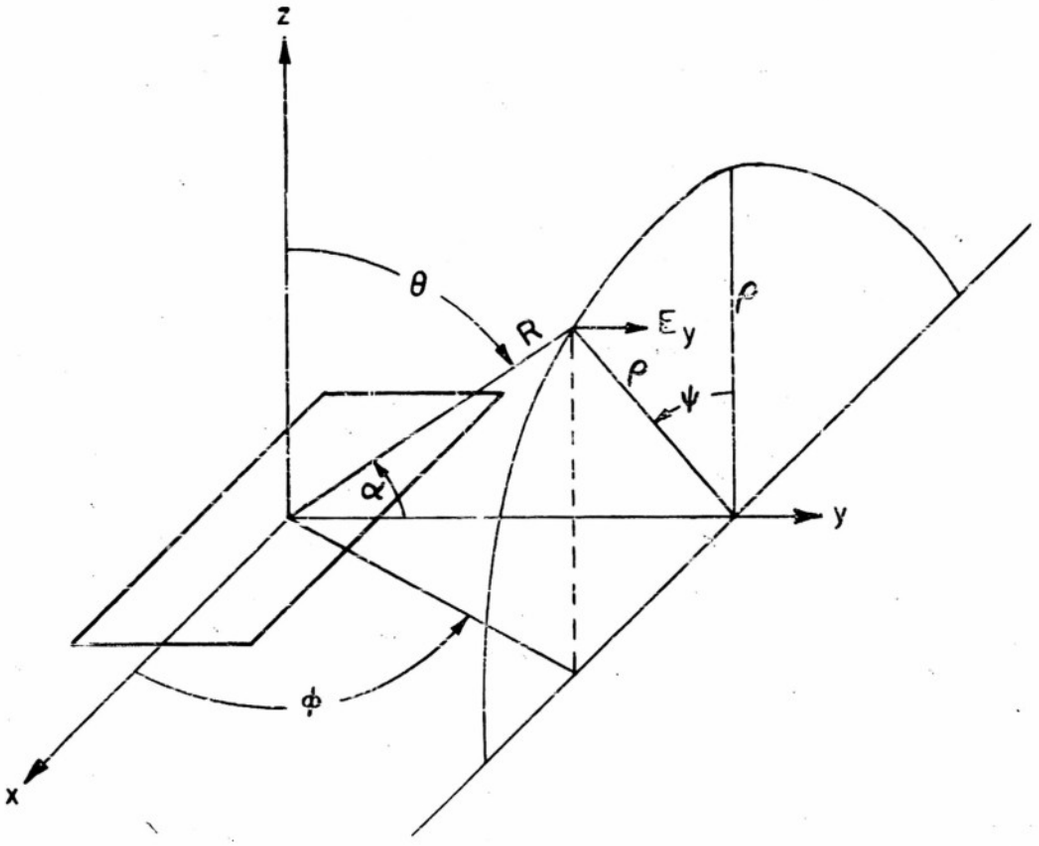

$$\sin\theta\cos\phi = \sin\alpha\sin\psi$$
$$\sin\theta\sin\phi = \cos\alpha$$
$$\cos\theta = \sin\alpha\cos\psi$$

Fig. 2

SYSTEM OF COORDINATES TO OBTAIN E_y AT CONSTANT ANGLE α

III. Experimental Procedure

Far zone patterns were taken with the waveguide fed aperture mounted flush in a 5' x 6.6' ground plane. The receiving horn and bolometer detector were mounted on a rotatable U frame 5.9 feet above the ground plane. The U frame was synchronized to a polar recorder.

Probe Measurements:

Figure (3) is a photo of the apparatus used in taking amplitude measurements in the slot. The probe carriage and bolometer detector assembly is isolated from the aperture to the extent of 40 db. by means of polyfoam strips sprayed with Aquadag solution[6]. The sprayed strips are supported in two transverse columns so as to absorb both polarization components. The presence of the complete assembly, except for the probe and supporting coaxial line, was found to have no effect on a surface probe placed in the aperture. The apparatus thus provided a convenient support for the moving probe and eliminated the danger of stray pickup at the detector assembly, while causing no distortion of the aperture field. The extent of aperture field distortion due to the presence of the probe and adjacent coaxial line remains an unknown factor.

Of the various probes investigated, the slot fed dipole was found to be the most satisfactory. It is the least bulky, has good pickup and symmetry, and is the easiest to make since no balun is necessary.

Measurements of $E_y(x)$ were made with a slot fed probe of a quarter wavelength total dipole length, 1/16" outer diameter coaxial line, and .010" slot width. The short dipole structure was necessary since E_y reverses phase at the center of the half wavelength wide slot. Measurement of $E_y(x)$ does not require probe symmetry. However, extraneous pickup did alter the relative readings when a set of readings was taken with the probe rotated 180 degrees. Since it

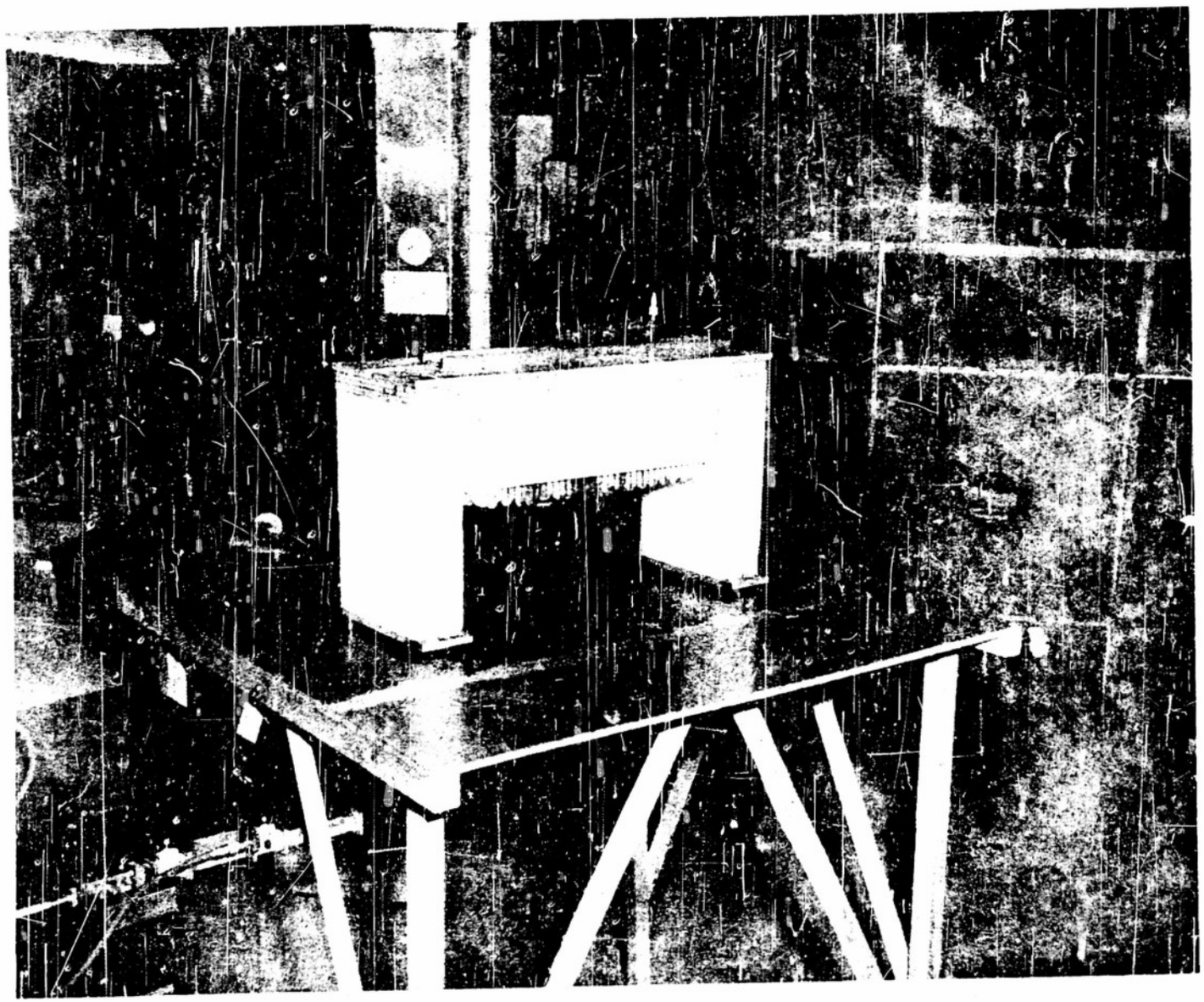

was not known which of the two probe positions was least subject to this extraneous pickup, it was decided to take two runs and to average the readings. The probe was rotated 180 degrees for each run. Averaging at least gave a mean between the largest and smallest error.

Preliminary measurements of $E_x(x)'$ for the case $a = \lambda$ were of such a perplexing nature it was decided to use two different probes (a slot fed probe and a shielded two wire line probe) in order to help clarify the type of probe errors being encountered. The slot fed probe had a total dipole length of a half wavelength, a 1/16" outside diameter coaxial line and .010" width slots. The shielded two wire line probe had a quarter wavelength total dipole length, and 1/32" outside diameter copper shielding for each half dipole lead. Neither probe displayed ideal symmetry so the same averaging procedure was followed in making the measurements for $E_y(x)$.

Synthesis Procedure:

Synthesis of the aperture distribution to approximate the measured aperture field or to give a far zone field that correlates with the measured far zone pattern is more easily done graphically. For the larger apertures, where 3 or 4 standing wave modes may be present, graphical computation is the only practical method. Because of errors in measurement, the use of matrices to obtain the mode constants from experimental data yields unsatisfactory results.

The pattern integrals used are shown in the appendix. The particular form shown for the pattern due to the traveling wave modes is convenient for graphical computation.

IV. Results and Discussion

Best results were obtained for E_y, on which the major part of the discussion will be centered.

The half sine form of $g_2(y)$ (equations 2 and 3) integrates to give the far zone pattern shown in graph (2). This pattern agrees to 2% with the measured patterns in the plane $\phi = 90$ degrees for the entire range of dimensions investigated. Because of the transverse dimension of the slot the experimental data serve only to verify the existence of the null in $g_2(y)$ along the central line and the amplitude symmetry about the null.

E_y as a Traveling Wave Mode:

The two-wavelength slot, whose far zone pattern has all the appearances of a traveling wave type of pattern was considered first. The phase and attenuation constants were obtained from the diffraction pattern as follows:

(a) Assume that the amplitude of the reflected wave in the slot is of such small magnitude that it has no effect on the angle of the maximum of the main lobe produced by the positively traveling wave. Examination of equation (13) in the appendix shows that the angle ψ at which $E_y/\cos\psi$ is a maximum determines the phase constant β by the relations:

$$\frac{c}{v} = \sin\alpha \sin\psi$$
$$\beta = \frac{c}{v} k \qquad (11)$$

where: $\frac{c}{v}$ = ratio of free space phase velocity to the phase velocity of the traveling wave in the slot

k = phase constant of a traveling wave in free space

$\sin\alpha$ is determined by the position of the receiving horn.

For all measurements, $\sin\alpha = .875$

(b) Knowing the phase constant, use equation (13) to determine an angle ($-\psi$) close to the main lobe of the negatively traveling wave at which E_y due to the positively traveling wave is a minimum. Obtain the relative amplitudes of the measured E_y at $-\psi$ and $+\psi$. The attenuation constant is then obtained from the relation:

$$\frac{E(+\psi)}{E(-\psi)} = \frac{1}{e^{-\alpha L}} \qquad (12)$$

By this method, a value of $\frac{c}{v} = .475$ and an attenuation constant $\alpha = .125$ nepers per cm. were obtained for the two-wavelength slot. Graph (9) shows good agreement between calculated and measured patterns. Once obtained, these same values should hold for the shorter slots as well. However, the best synthesis of the far zone patterns for the shorter slots required slightly smaller phase and attenuation constants. Good agreement with the patterns for the slot lengths from $7\lambda/4$ to $\lambda/2$ was obtained for a $\frac{c}{v} = .45$, and an $\alpha = .096$ nepers per cm. Measured and calculated patterns are shown in graphs (3) to (8).

For slot lengths of 1.5 wavelengths or less, method (a) did not hold since the rear lobe of the negatively traveling wave affected the tilt angle of the main lobe for the positively traveling wave. However, the values obtained for the 7/4 wavelength slot also gave good pattern correlation for the shorter slots, thus avoiding the necessity of making successive approximations to the unknown phase velocity and obtaining the attenuation constant by method (b) for each approximation until satisfactory correlation between measured and computed patterns is obtained.

The aperture distribution determined by these mode constants is compared with the measured distributions in graphs (11) to (14). Here, no agreement is

seen to exist.

E_y as a Sum of Standing Wave Modes:

The standing wave mode hypothesis yields more satisfactory correlation between the measured aperture distributions and those synthesized from the far zone patterns. The aperture distributions arrived at are listed below in order of increasing slot length. The 1.5 wavelength slot has a second, less likely distribution listed in parenthesis. It is used to illustrate the different effects produced on the far zone and slot fields when a third mode is introduced.

Table I

Slot Length a in Wavelengths	Slot Field Distribution $f_2(x)$
1/2	$\cos \frac{\pi x}{L}$
3/4	$\cos \frac{\pi x}{L} + .1 e^{-j90} \sin \frac{2\pi x}{L}$
1	$\cos \frac{\pi x}{L} + .2 e^{-j37} \sin \frac{2\pi x}{L}$
5/4	$\cos \frac{\pi x}{L} + .7 e^{-j29} \sin \frac{2\pi x}{L}$
3/2	$(\cos \frac{\pi x}{L} + 1.55 e^{-j35} \sin \frac{2\pi x}{L})$
	$\cos \frac{\pi x}{L} + 1.55 e^{-j35} \sin \frac{2\pi x}{L} + .15 e^{-j90} \cos \frac{3\pi x}{L}$
7/4	$\cos \frac{\pi x}{L} + 4 e^{-j80} \sin \frac{2\pi x}{L} + 1 e^{j35} \cos \frac{3\pi x}{L}$
2	$\cos \frac{\pi x}{L} + 4 e^{-j110} \sin \frac{2\pi x}{L} + 2 e^{j25} \cos \frac{3\pi x}{L} + .75 e^{-j45} \sin \frac{4\pi x}{L}$

Phase angles are in degrees.

The far zone and aperture fields for the above listed distributions are compared to the measured far zone and aperture fields in graphs (3) to (9) and

graphs (11) to (14), respectively. The correlation is seen to be much better than that obtained with the traveling-wave-mode hypothesis.

The slot field distribution was obtained from synthesis of the far zone patterns for slot lengths from 1/2 wavelength through 5/4 wavelength. The third mode for the 3/2 wavelength slot was arrived at with some attention being given to the measured slot distribution. Sufficient confidence was had in the probe readings by the time the 7/4 wavelength slot was investigated so that it was decided to obtain the distributions for the 7/4 and 2 wavelength slots by working jointly with both the far zone patterns and the probed distribution. Because of the many modes in the 2 wavelength slot, a solution giving good correlation between the aperture and far zone measurements would have been most difficult without using the two together in the synthesis of the aperture field.

Each slot length will be discussed briefly:

Graph (11a) shows only a correlation for the case of the half wavelength slot. However, the field perturbation due to the presence of the probe and its coaxial support would be expected to be large in such a small aperture. In addition, results for the larger size slots consistently show a high extraneous probe pickup in the 1/4 wavelength region near the end of the slot. In the 1/4 wavelength region at the beginning of the slot, the extraneous pickup is consistantly only about one fourth as high. This explains the asymmetry in the probe readings for the half wavelength aperture.

The 3/4 wavelength slot appears to have a small asymmetry in the far zone pattern. However, the radiated energy in E_y is so low for the 3/4 wavelength slot (as well as for the half wavelength slot) that pickup of stray reflections from discontinuities in the ground plane and from the structure supporting the receiving horn tends to cloud the true pattern. The slot is too short to

allow sufficiently accurate probe readings in the neighborhood of the aperture to determine the absence or presence of a second mode of excitation. The pattern asymmetry was accepted for mode synthesis but the conjecture would be that the 3/4 wavelength slot has only a single mode. Otherwise the relative amplitude of this second mode for the one wavelength slot would be expected to be higher than observed.

The decrease of probe errors with increasing slot length is illustrated in graphs (12a) and (12b).

Graph (13a) shows that two modes give a relatively poor correlation with the probe measurements for the 3/2 wavelength slot. Better agreement is obtained by the addition of a third mode. The disparity in the data about the minimum can be partly attributed to extraneous pickup. Another possible explanation for the mediocre correlation, even with three modes, is that these readings were taken before it was decided to average the readings from two runs. (Probe reversed 180° for second run.) Graph (7) shows the minor effect of the third mode on the far zone pattern.

The good correlation for the 7/4 wavelength and the two-wavelength slots can be attributed to reduced probe errors, to the joint utilization of both far zone and aperture fields for obtaining the mode constants, and to an improved technique obtained from experience with the smaller slots. Although the far zone pattern for the 2 wavelength slot could be accounted for satisfactorily by only three modes, a fourth mode was required for a satisfactory representation of the measured aperture field distribution.

A comparison of the results obtained with the traveling wave hypothesis and the standing wave hypothesis can only lead to the conclusion that the latter hypothesis is more accurate. In fact, the close correlation between the

synthesized aperture field and that determined by probe measurements leads to the belief that the standing wave hypothesis holds exactly for slot lengths between 1/2 wavelength and two wavelengths. Of course, a study of the phase characteristics of the field are needed to substantiate this hypothesis more fully.

An estimate of the accuracy of the mode constants obtained would be $\pm$ 10% for the amplitude constants and $\pm$ 5 degrees for the relative phase values.

Graph (15) shows the phase curves for the field distributions in the 7/4 wavelength slot obtained by both the standing wave and the traveling wave methods. The similarity of the curves explains why it was also possible to obtain good pattern correlation with an assumed traveling wave mode in the aperture. The likeness is even more marked if the minimum amplitudes are taken as reference points and made to coincide on the graph. The horizontal lines in graph (15) indicate the traveling wave minimum at x = -.7 cm. and the standing wave minimum at x = + .06 cm. A comparison of phase curves for the other length slots would be expected to be equally similar. A check on the 1/2 wavelength slot shows a traveling wave phase variation of only -4° from x = - .8 cm. to x = 0 (region of large field amplitude), and a phase variation of $+ 6^\circ$ from x = 0 to x = + .8 cm. (region of small field amplitude). The standing wave phase variation is zero for the single cosine mode in the 1/2 wavelength slot.

E_x Polarization:

Probe measurements for all slot lengths, including the 3 wavelength slot, consistently show a reversed J type of amplitude distribution. Pattern measurements show an increasing number of side lobes with increasing slot length. The large height and the periodicity of these side lobes indicates the presence of spurious radiation from the slot edges at x = - a/2 and x = + a/2.

The three wavelength slot displays aperture and far field characteristics similar to those of the two wavelength and shorter apertures. Because of the greater number of interference lobes and the larger region over which probe measurements can be made, the three wavelength aperture is the most convenient for analysis of the edge field radiation. The measured far zone and aperture fields are shown, respectively, in Graphs (10) and (16).

The aperture field in Graph (16) has an appearance more like a traveling wave mode with a high attenuation constant rather than that of a combination of a limited number of standing wave modes. However, the far zone field shown in Graph (10) is obviously not a pattern due to a traveling wave plus a reflected wave mode. Expressing this measured aperture field as a summation of standing wave modes would require a great number of modes. Such a solution has not been attempted since it is outside the realm of our finite mode hypothesis.

Since the far zone pattern cannot be obtained from the traveling wave mode hypothesis and since the aperture distribution cannot be synthesized by the finite standing wave mode hypothesis, a reliable solution that gives correlation between the aperture and far field measurements is unattainable with either hypothesis alone. Having established the standing wave mode hypothesis for the $E_y(x)$ aperture fields, a logical step was to attempt to express the $E_x(x)$ fields as a superposition of standing wave modes plus high amplitude edge fields. However, an attempt at obtaining the form of the edge fields leads to contradictory results which, once more, minimizes the possibility of obtaining good correlation between the aperture and far field measurements. Examination of Graph (16) shows that a traveling wave with an attenuation constant of 0.9 nepers per cm. gives a good approximation to the measured edge fields. The absence of aperture phase measurements leaves only far zone patternsas the means for obtaining the

phase characteristics of the edge fields. From a mode concept, the discontinuity presented to the dominant waveguide mode by the aperture is expected to give rise to a number of higher order evanescent modes. Where the aperture length is in the order of a wavelength or more, these higher modes will be localized in the region of the aperture edges at $x = \pm a/2$. The proximity of the aperture edge fields to these evanescent waveguide fields suggests that the edge fields also have an infinite phase velocity. However, an attempt at approximating the positions of the maxima and minima of the measured far field interference lobes by assuming the presence of edge fields with 0.9 nepers per cm. attenuation and an infinite phase velocity was unsuccessful. Reasonable agreement was found to require an attenuation constant of 5.3 nepers per cm. But this large value affords no correlation with the measured edge fields. It is unlikely that edge fields characterized by a finite phase velocity and by the measured attenuation constant of 0.9 nepers per cm. would result in a more successful synthesis of the far field pattern, so further investigation was discontinued at this point.

Good agreement with the observed side lobe minima and maxima for slot lengths from three wavelengths to one wavelength (the 3/4 and 1/2 wavelength slots have no side lobes) can be obtained by approximating the fields at the edges of the slot by sources of constant amplitude and phase extending from $x = -a/2$ to $x = -a/2 + \lambda/8$ and from $x = +a/2$ to $x = +a/2 - \lambda/8$ added to standing wave modes. The interference pattern for the three wavelength slot is shown in graph (10). The maxima and minima points are seen to agree except about the region of the directive main beam at $\theta = +35^{\circ}$. As mentioned previously, reasonable agreement with the maxima and minima can also be obtained for an assumed evanescent mode, of 5.3 nepers per cm. attenuation, at both slot edges. However, agreement was best with the step type of source and since neither gave particularly more satisfactory correlation with the probe readings, the step source was used.

V. Conclusion

Evidence has been presented indicating that the $E_y(x)$ aperture field, for slot lengths from 1/2 wavelength to two wavelengths, consists of one or more resonant standing wave modes. The number of modes resonating is a function of the slot length with respect to free space wavelength. For a slot of length $a = n\lambda/2$, where n is an integer, n resonant modes appear. The lowest order mode has a half period and the nth order mode has n/2 periods. Measurements have also been taken for the three wavelength slot. Calculations are incomplete but indications are that the standing wave hypothesis still holds. The dominate mode appears to be the $\sin \frac{4\pi x}{a}$ mode.

The $E_x(x)$ component of the aperture field distribution remains unclear. A solution first requires the determination of the form of the E_x fields in the region about the aperture edges. Phase measurements are necessary to clarify the phase behavior of the edge fields.

The good pattern synthesis obtained for $E_y(x)$ using the incorrect traveling wave mode hypothesis demonstrates the unreliability of amplitude pattern synthesis unless correlation with aperture amplitude measurements is also obtained. As a further example, reasonable synthesis of the far field patterns for the half wavelength square aperture could be obtained for each of the following $E_x(x)$ aperture distributions:

(1) A constant mode plus a half sine mode;

(2) A constant mode plus two aperture edge step sources;

(3) Only two aperture edge step sources.

However, none of these distributions is in good agreement with the measured aperture field.

Aperture lengths have not been reached at which the net $E_y(x)$ aperture field

changes from a summation of standing wave modes to a predominantly single traveling wave mode. A conjecture would place this critical aperture length between 4 and 5 wavelengths.

$E_\phi(\theta)$ IN THE PLANE $\phi = 90°$

$$E_\phi = \frac{\cos(\pi/2 \sin\theta)}{\cos\theta}$$

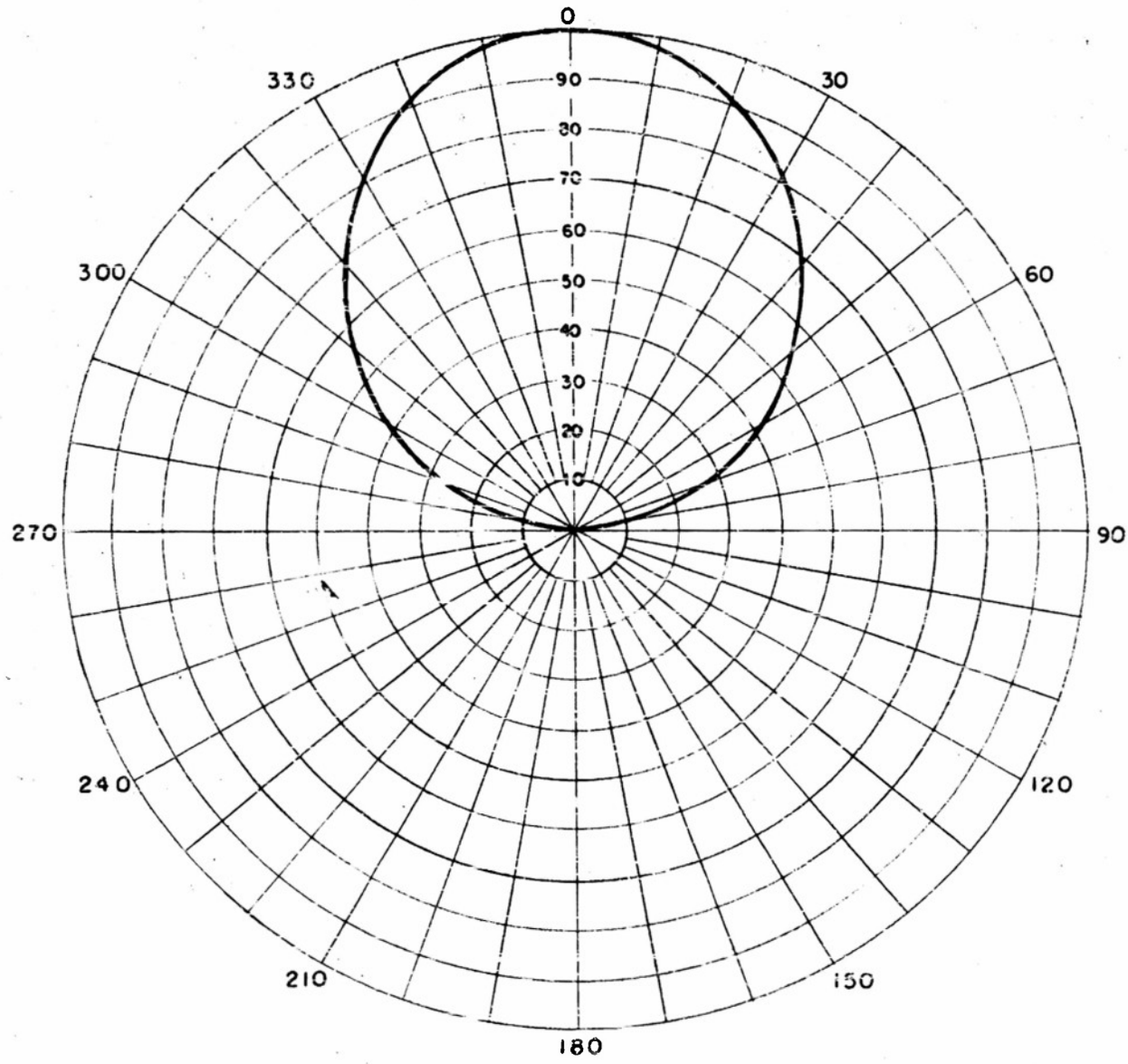

E_ϕ COMPUTED FROM APERTURE DISTRIBUTION $g_1(y) = \cos\frac{2\pi y}{\lambda}$

MEASURED PATTERNS FOR SLOT LENGTHS FROM 1/2 λ TO 3 λ AGREE WITH COMPUTED PATTERN TO MAXIMUM DEVIATION OF 3%

Graph 1

$E_\theta(\theta)$ IN THE PLANE $\phi = 90°$

$$E_\theta = \frac{\sin\theta \cos(\pi/2 \sin\theta)}{\cos^2\theta}$$

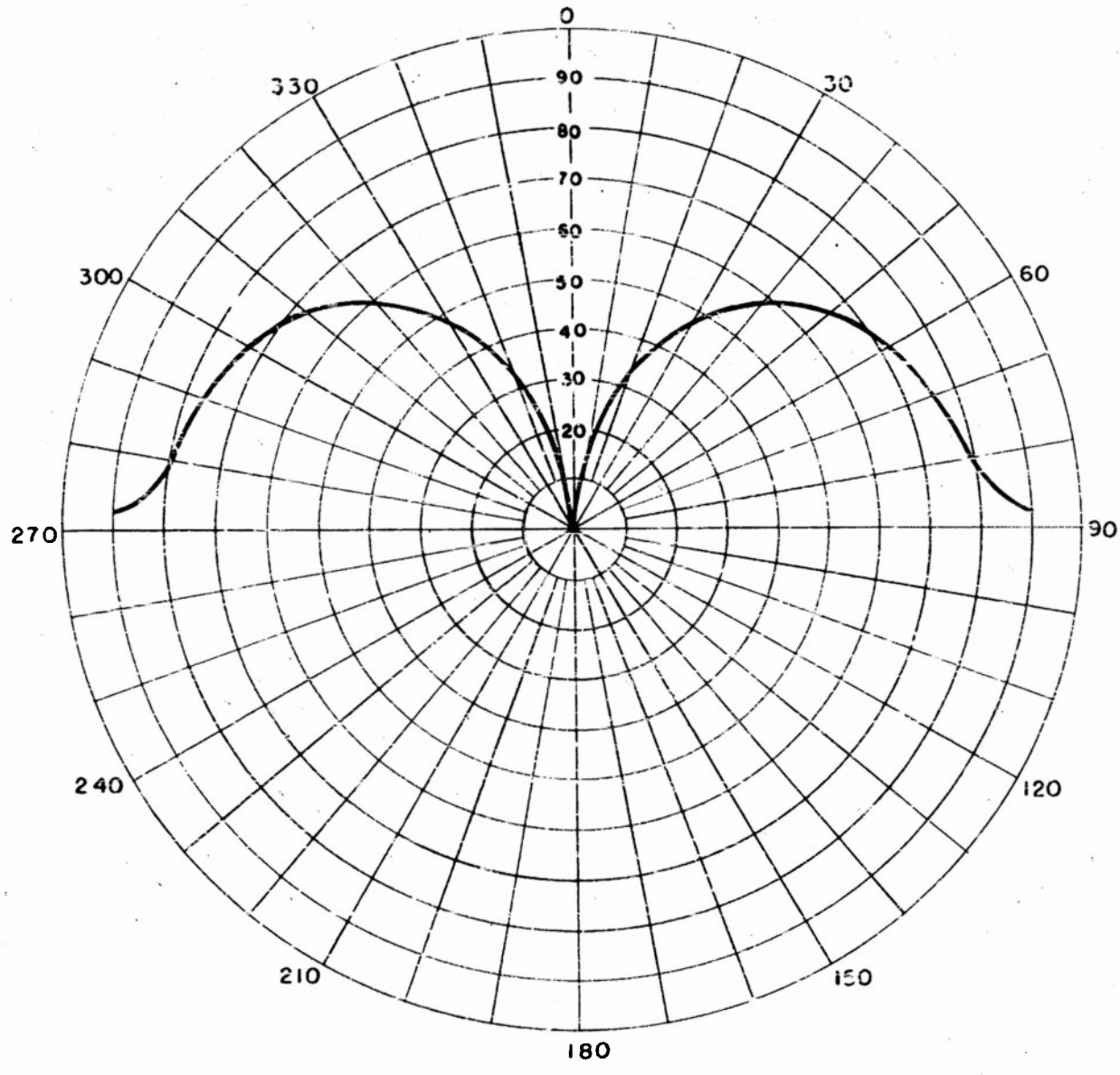

E_θ COMPUTED FROM APERTURE DISTRIBUTION $g_2(y) = \sin\frac{2\pi y}{\lambda}$

MEASURED PATTERNS FOR SLOT LENGTHS FROM 1/2λ TO 3λ AGREE WITH COMPUTED PATTERN TO MAXIMUM DEVIATION OF 5%

Graph 2

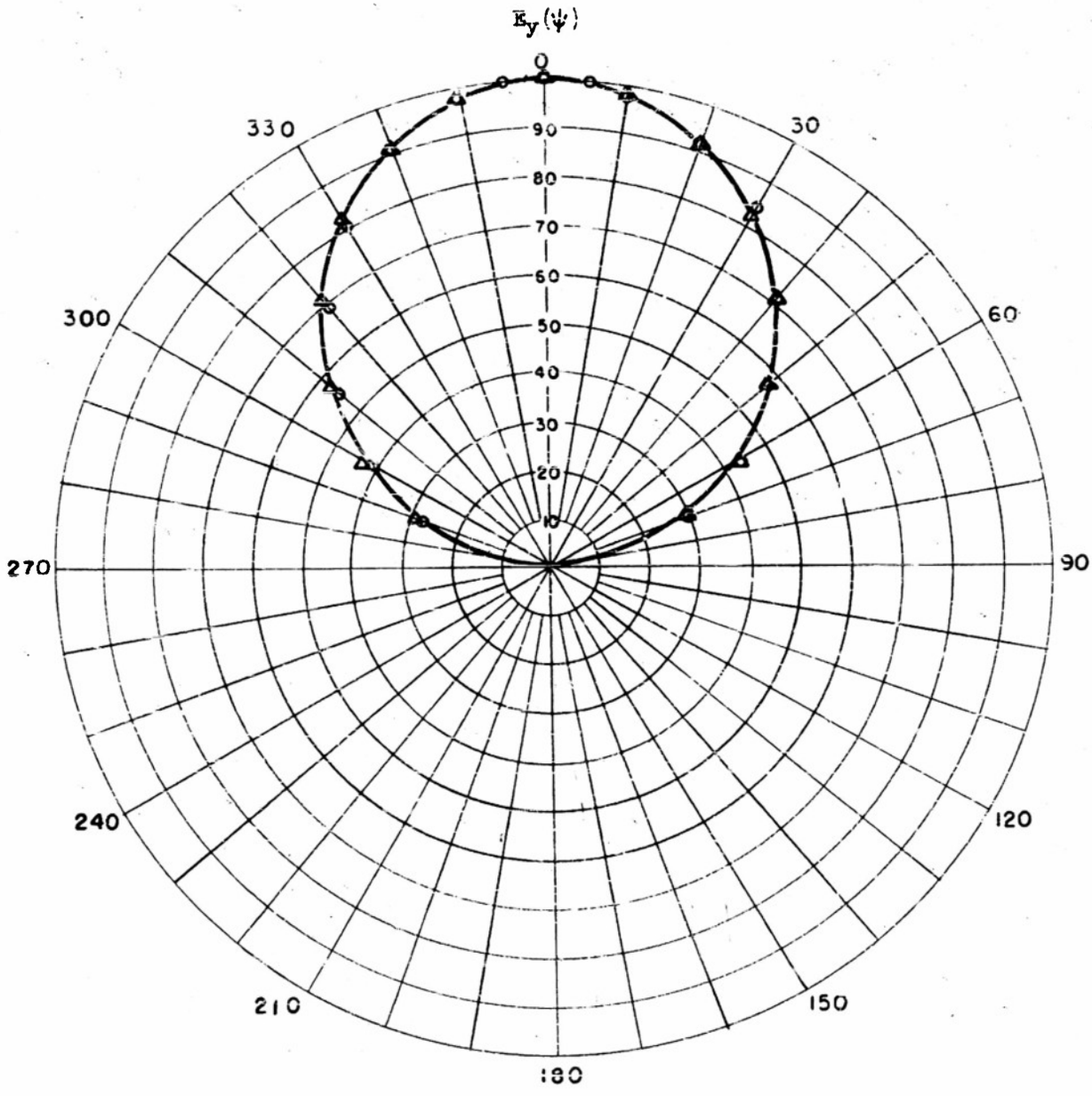

$a = \lambda/2$

——— MEASURED

△ STANDING WAVE, TABLE 1

○ TRAVELING WAVE
$\alpha\lambda = 0.306$, $c/v = 0.4$

Graph 3

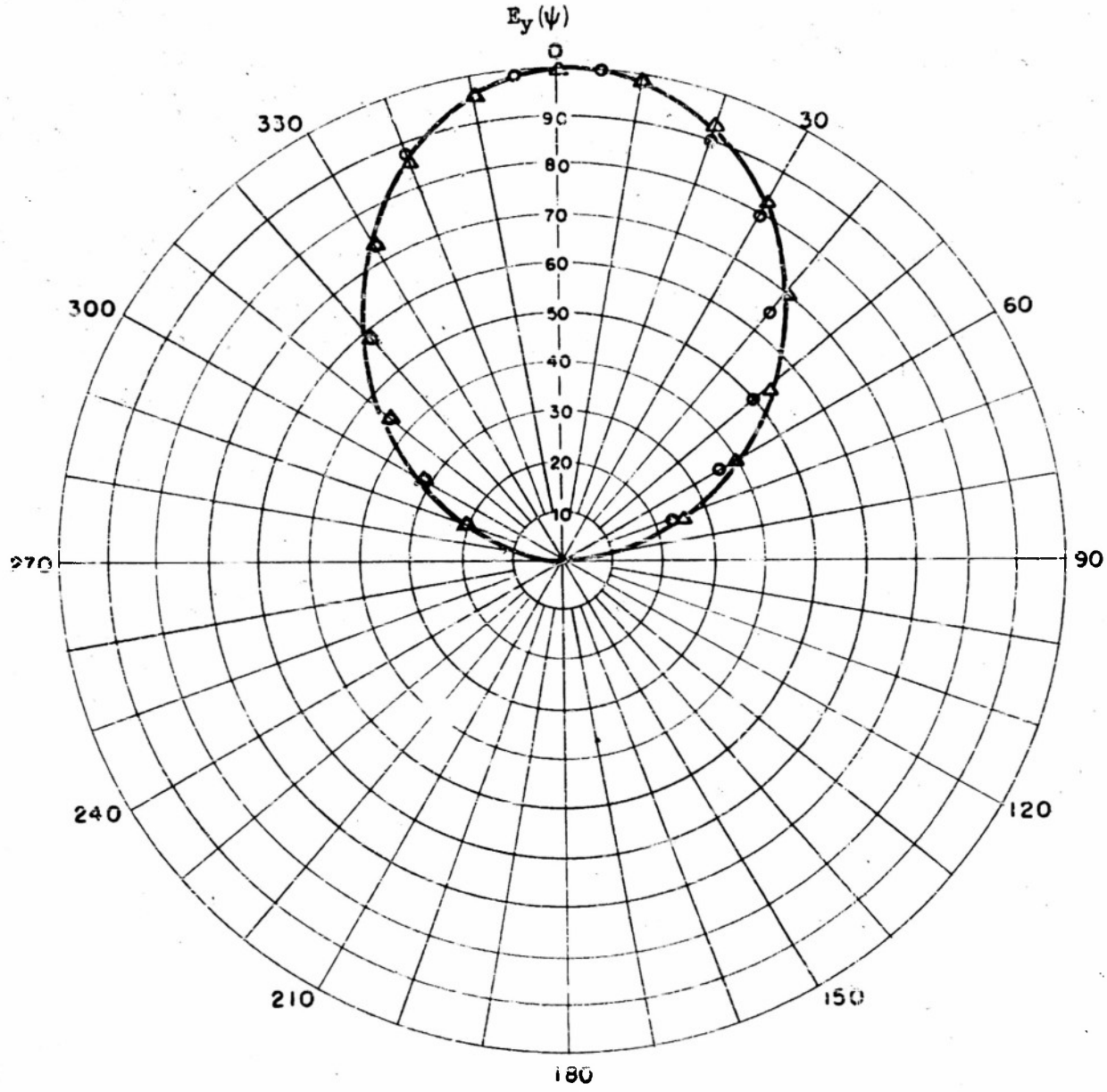

$a = 3\lambda/4$

——— MEASURED

△ STANDING WAVE, TABLE 1

○ TRAVELING WAVE $\alpha\lambda = 0.308$, $c/v = 0.45$

Graph 4

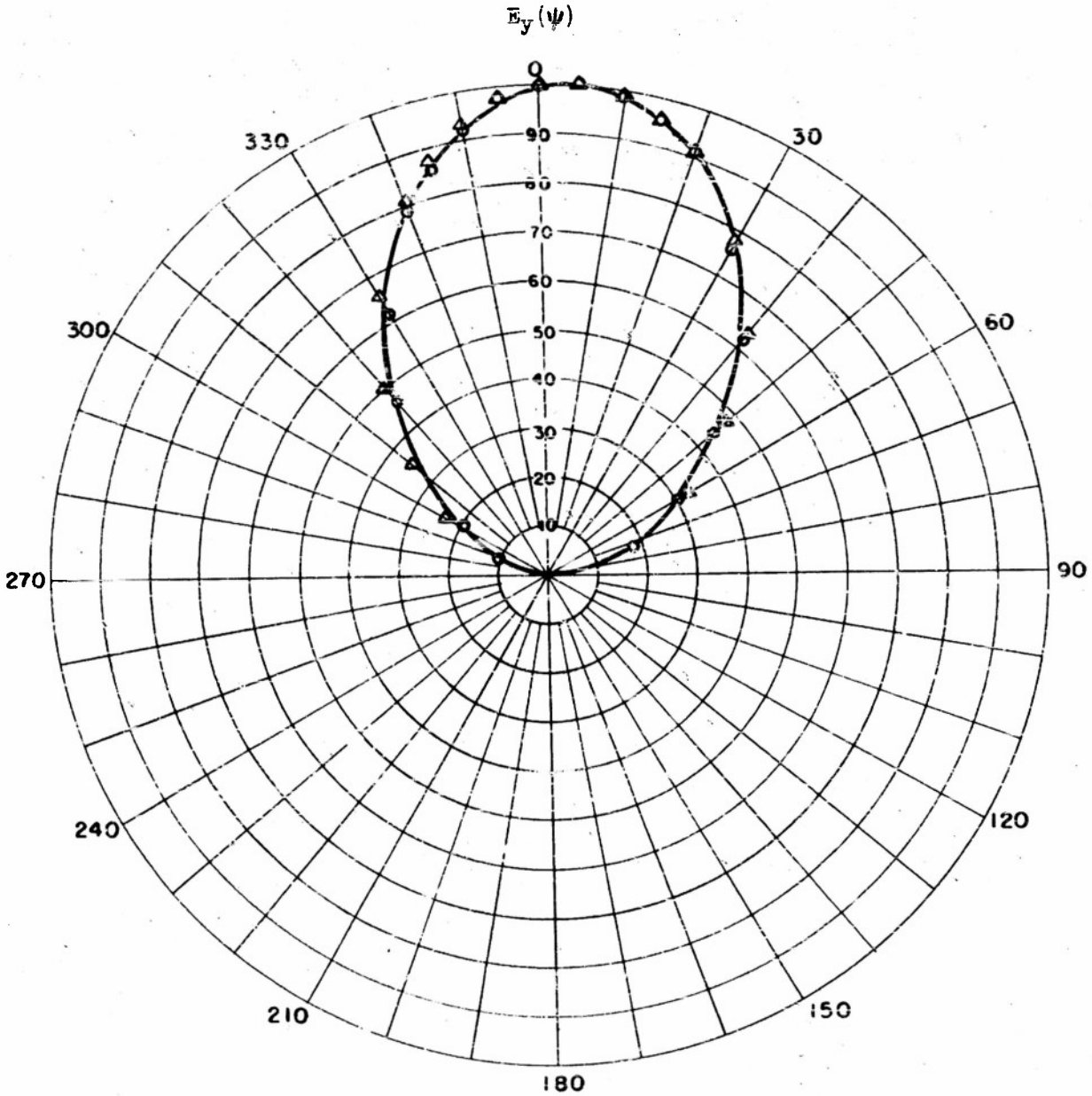

MEASURED

△ STANDING WAVE, TABLE 1

○ TRAVELING WAVE

$\alpha\lambda = .306$, $c/v = .45$

$a = \lambda$

Graph 5

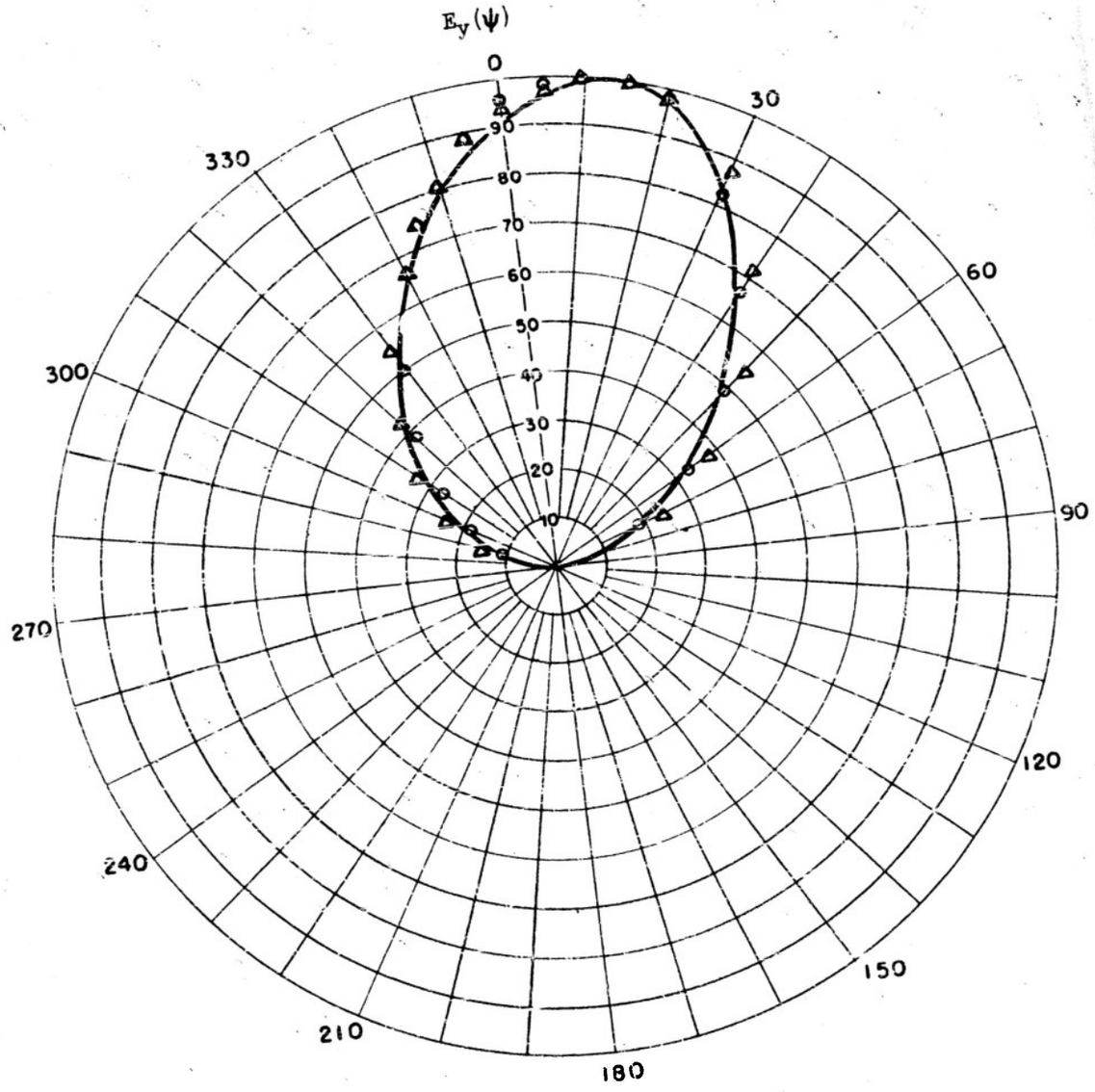
$E_y(\psi)$
0
30
60
90
120
150
180
210
240
270
300
330
10
20
30
40
50
60
70
80
90
MEASURED
STANDING WAVE, TABLE 1
TRAVELING WAVE
$\alpha\lambda = .306$, $c/v = .45$
$a = 5\lambda/4$

Graph 6

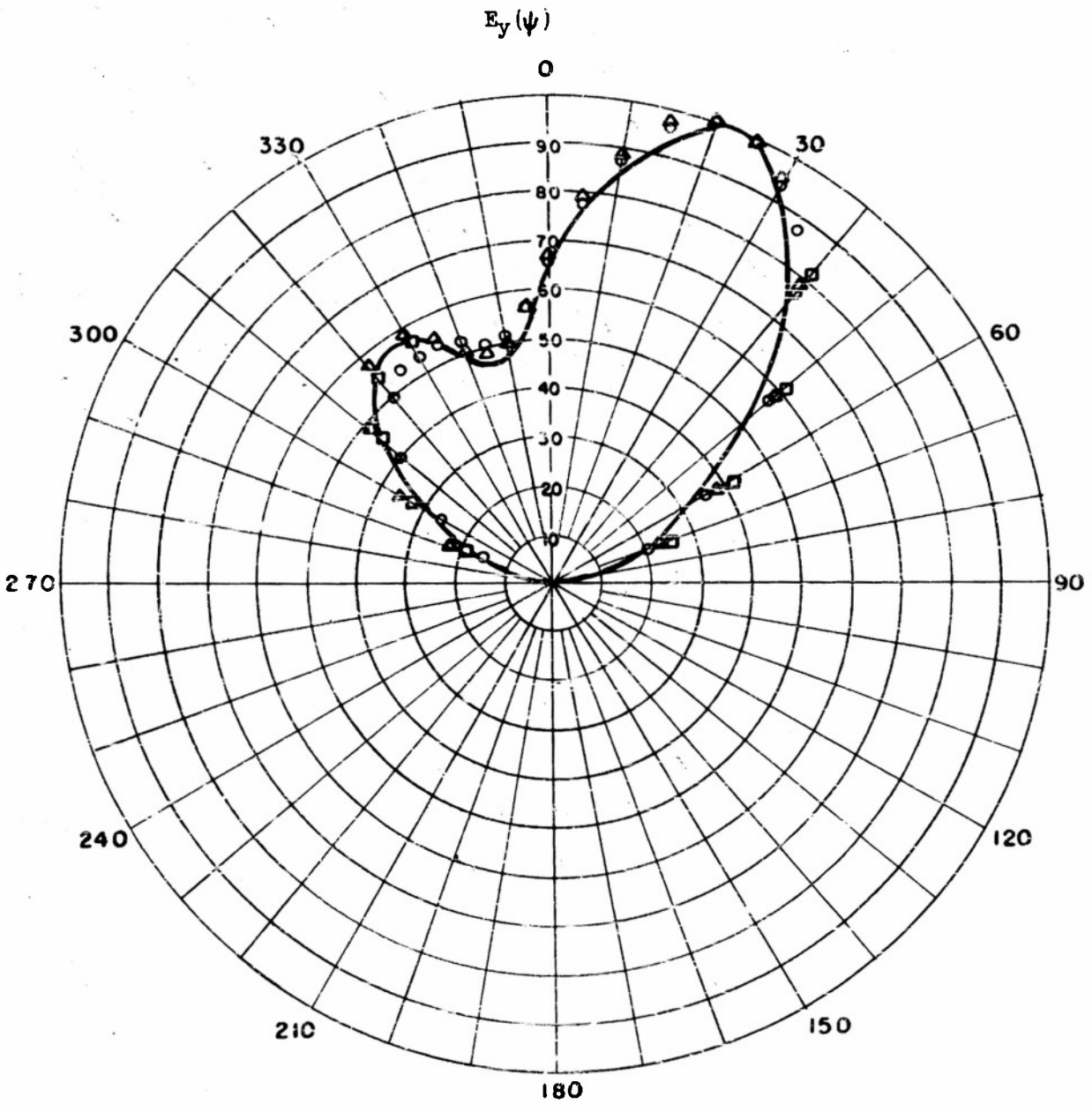

$a = 3\lambda/2$

MEASURED

△ STANDING WAVE, 3 MODES

□ STANDING WAVE, 2 MODES

○ TRAVELING WAVE $\alpha\lambda = .306$ $c/v = .45$

TABLE 1

Graph 7

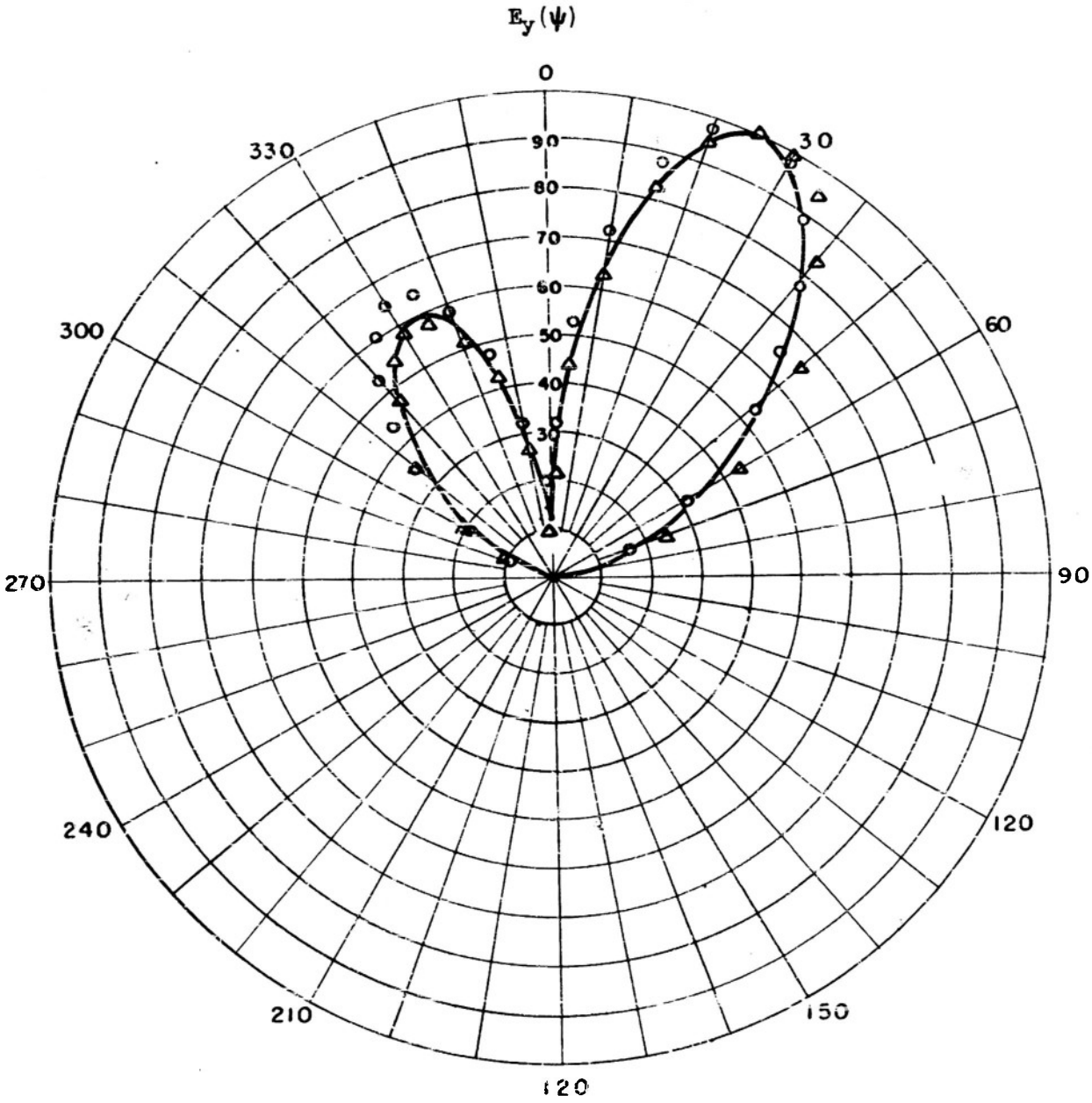

$a = 7\lambda/4$

——— MEASURED

△ STANDING WAVE, TABLE 1

○ TRAVELING WAVE, $\Delta\lambda = .306$, $c/v = .45$

Graph 8

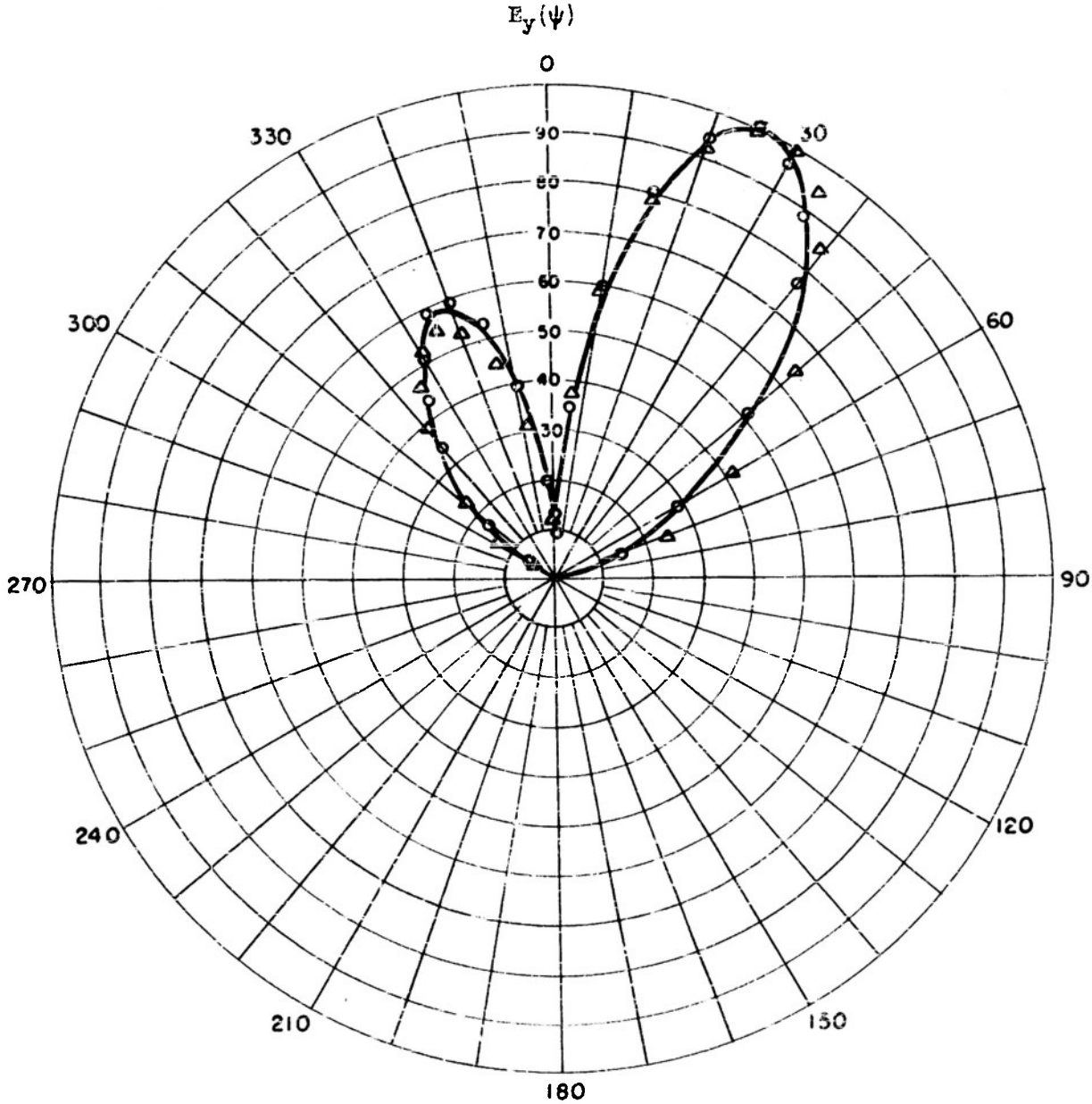

$a = 2\lambda$

Graph 9

$E_\theta(\theta)$
IN THE PLANE $\phi = 0$

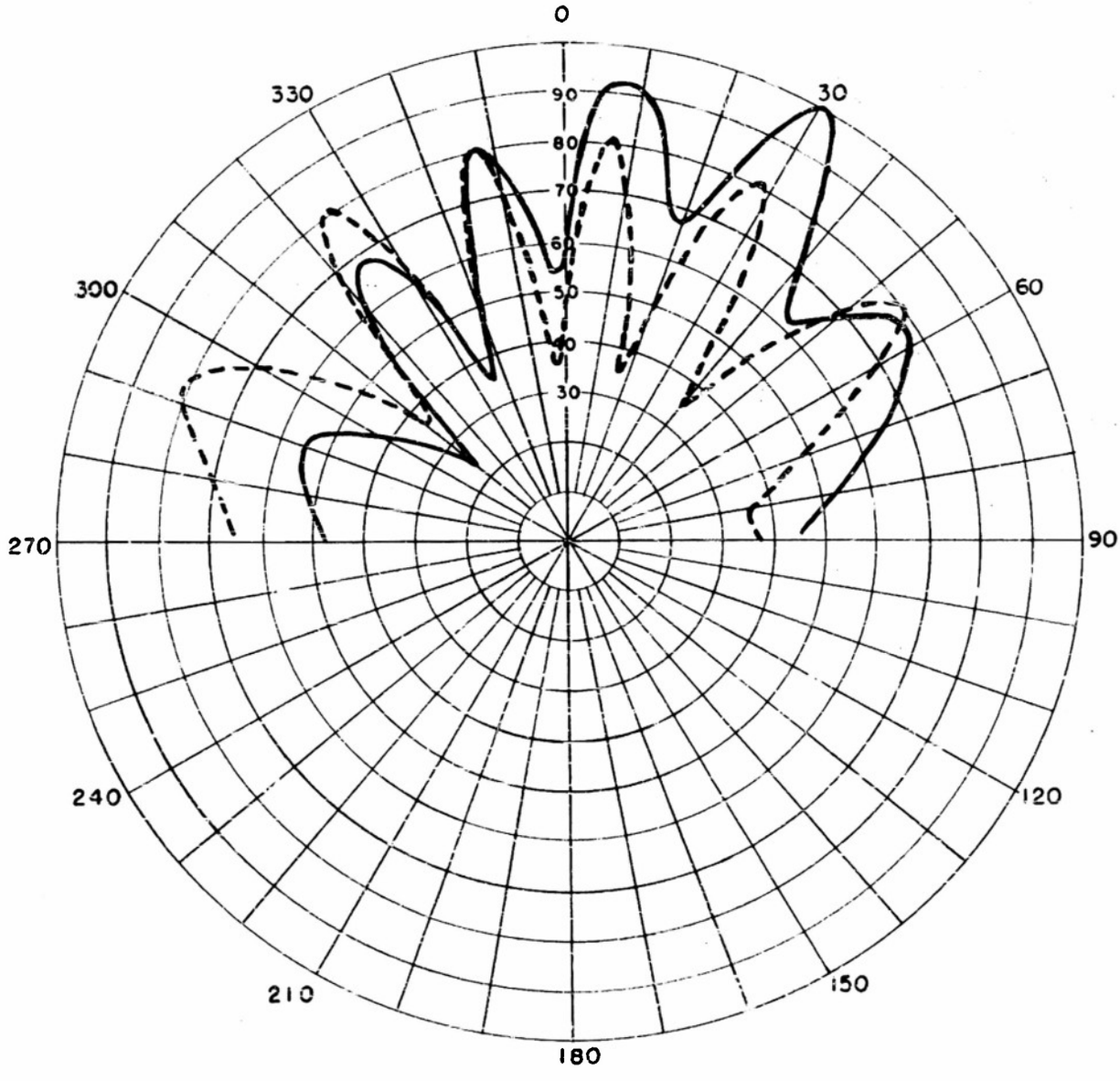

——— MEASURED

$a = 3\lambda$ – – – INTERFERENCE PATTERN DUE TO 1/8λ STEP SOURCES AT $x = \pm L/2$

Graph 10

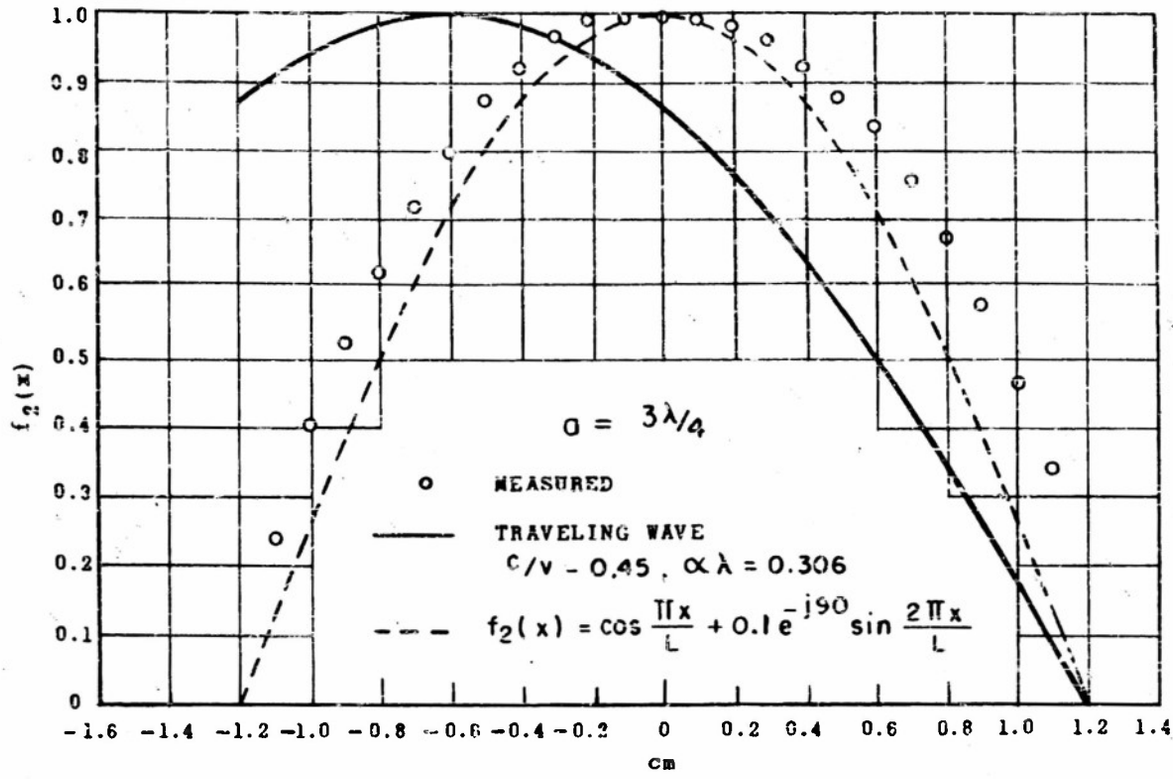

Graph 11b

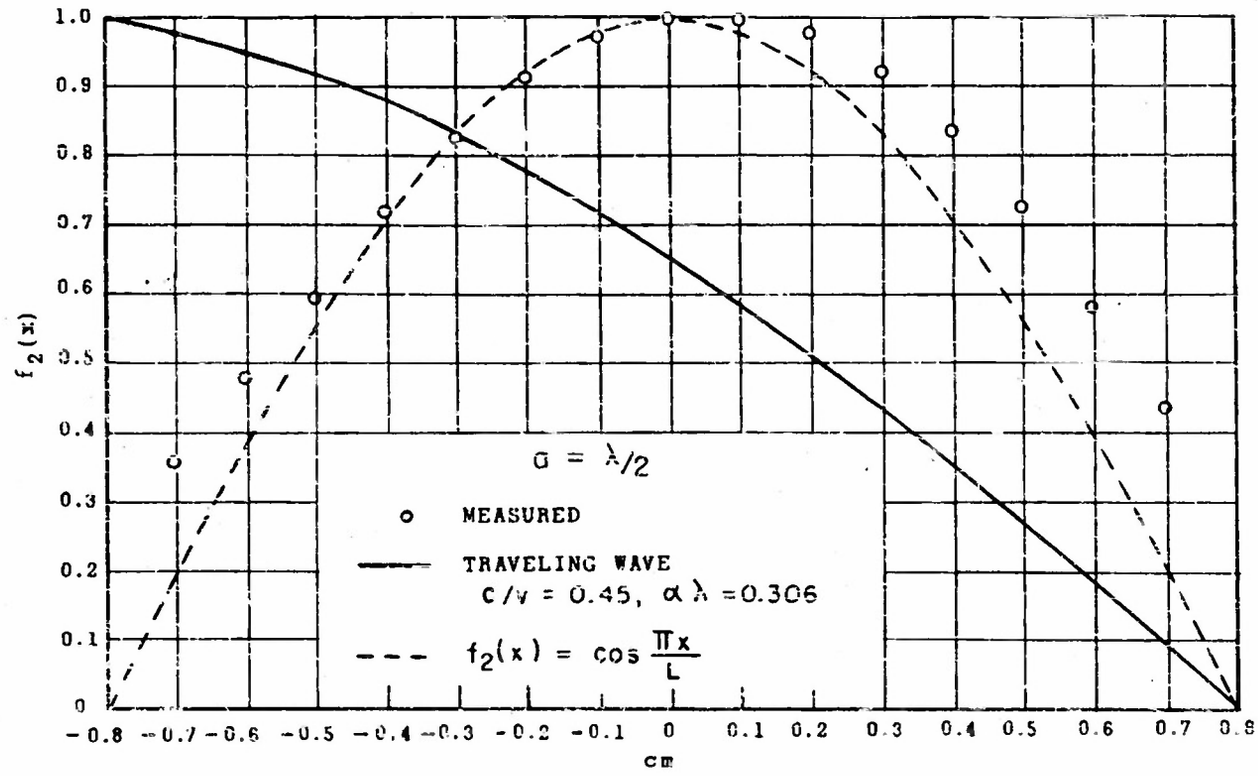

Graph 11a

E_y APERTURE AMPLITUDE DISTRIBUTION

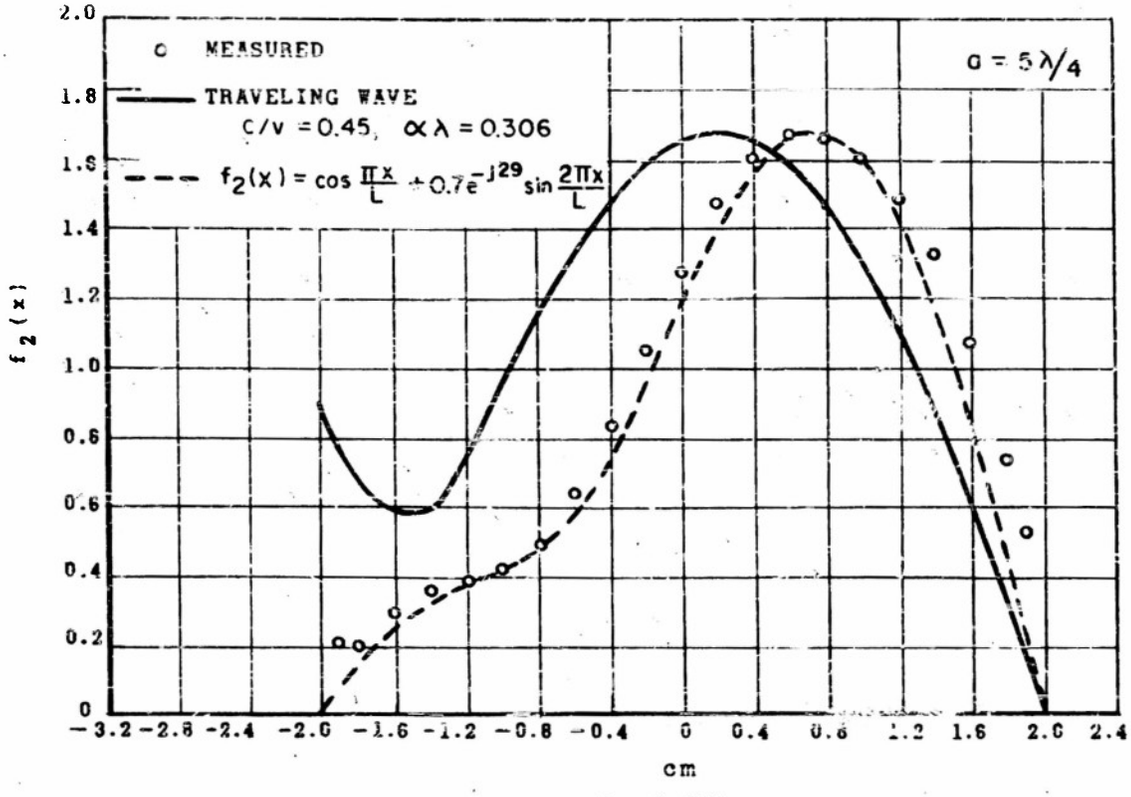

Graph 12b

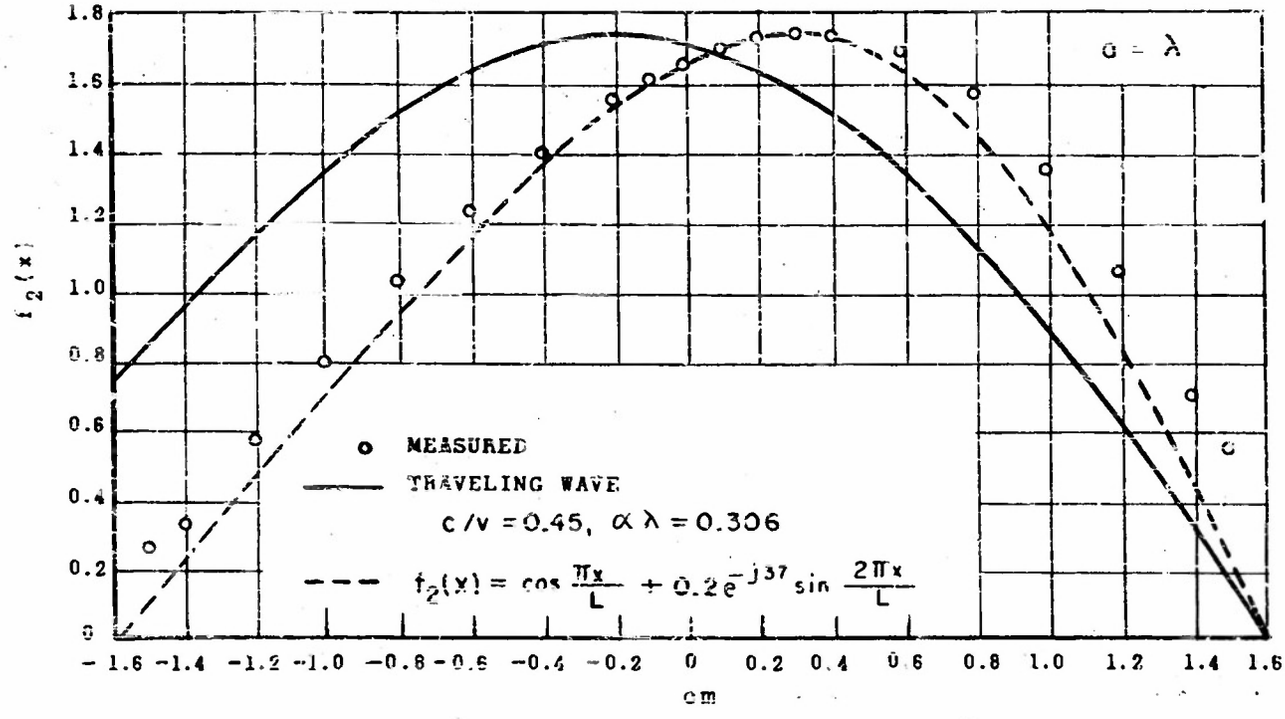

E_y APERTURE AMPLITUDE DISTRIBUTION

Graph 12a

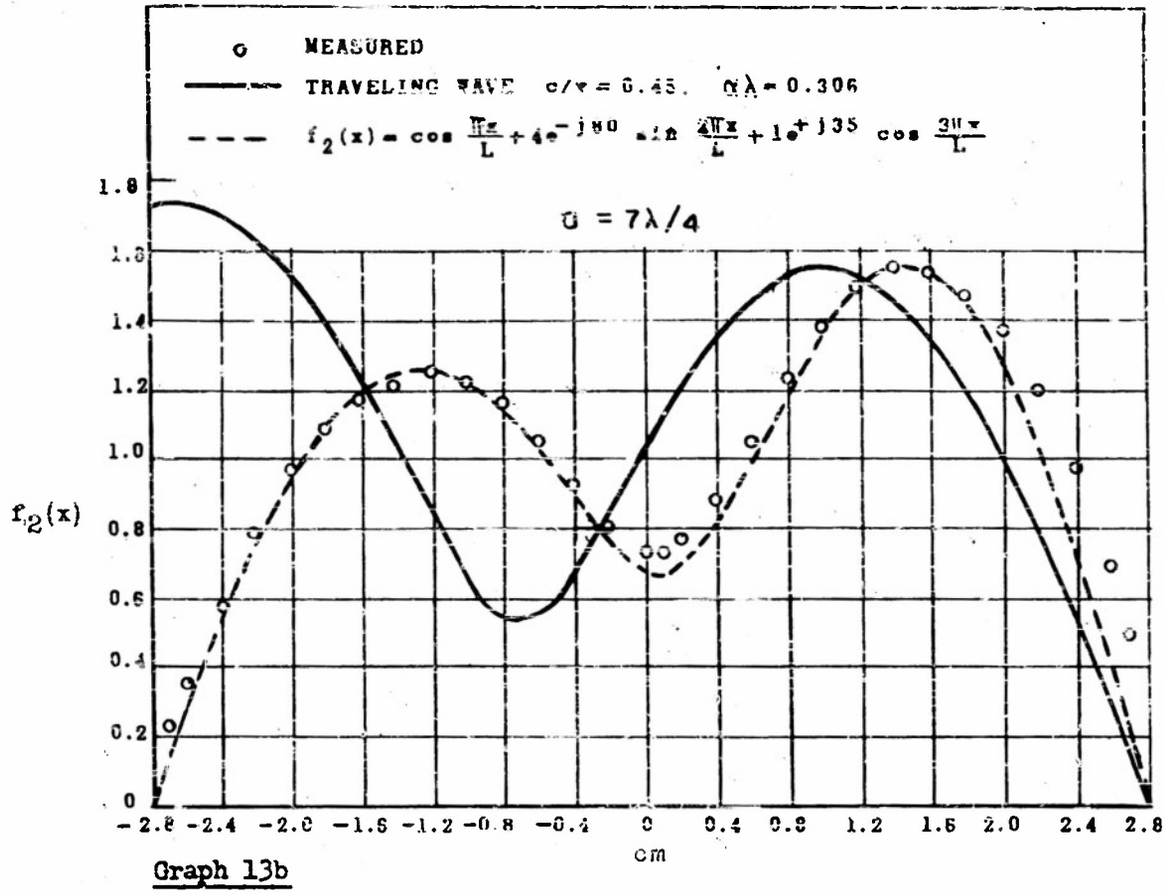

Graph 13b

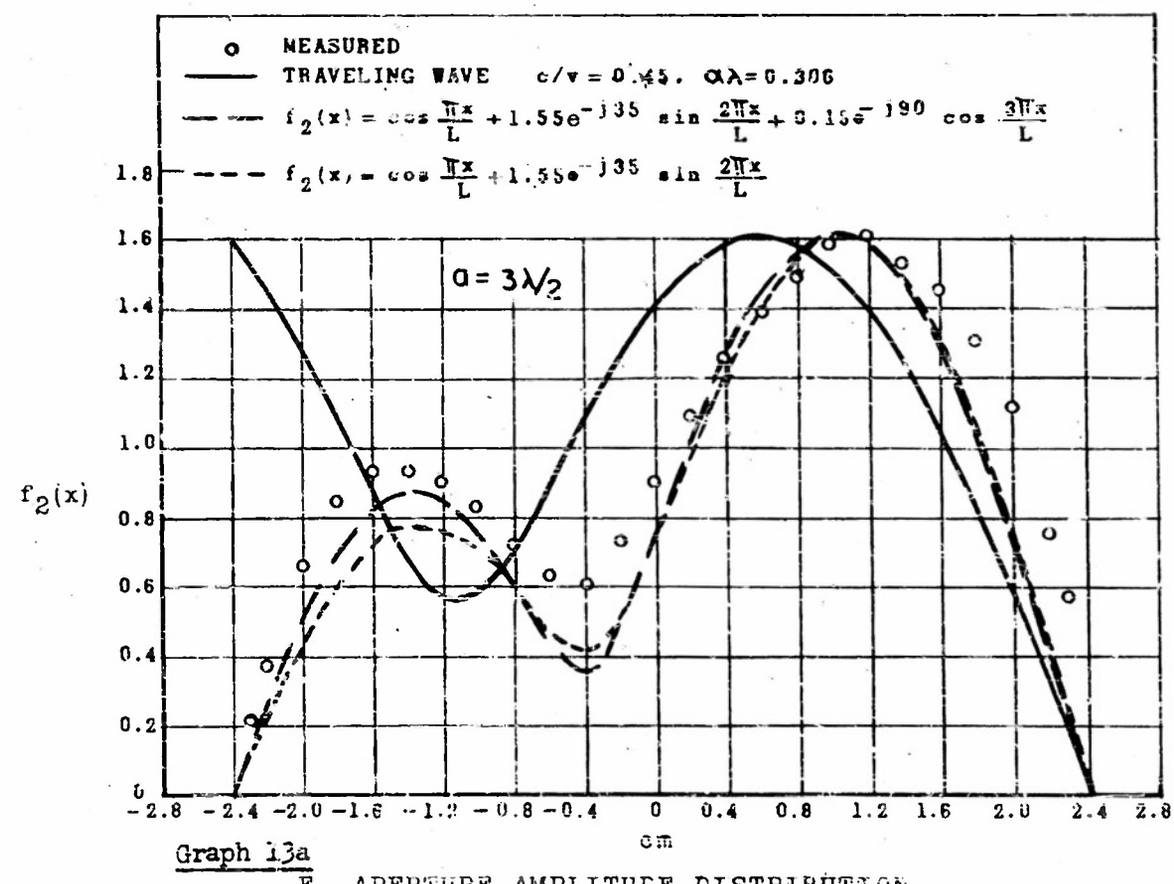

Graph 13a

E_y APERTURE AMPLITUDE DISTRIBUTION

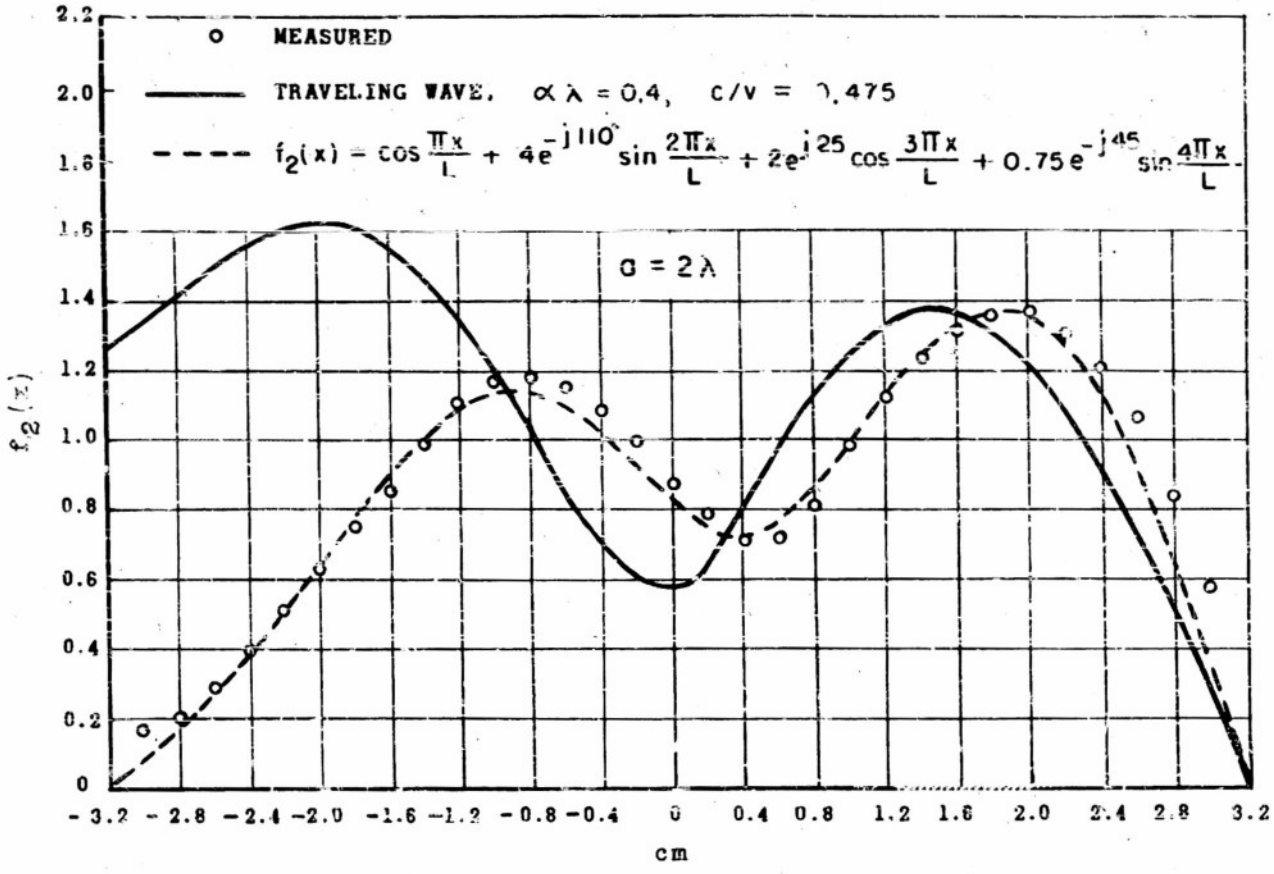

E_y APERTURE AMPLITUDE DISTRIBUTION

Graph 14

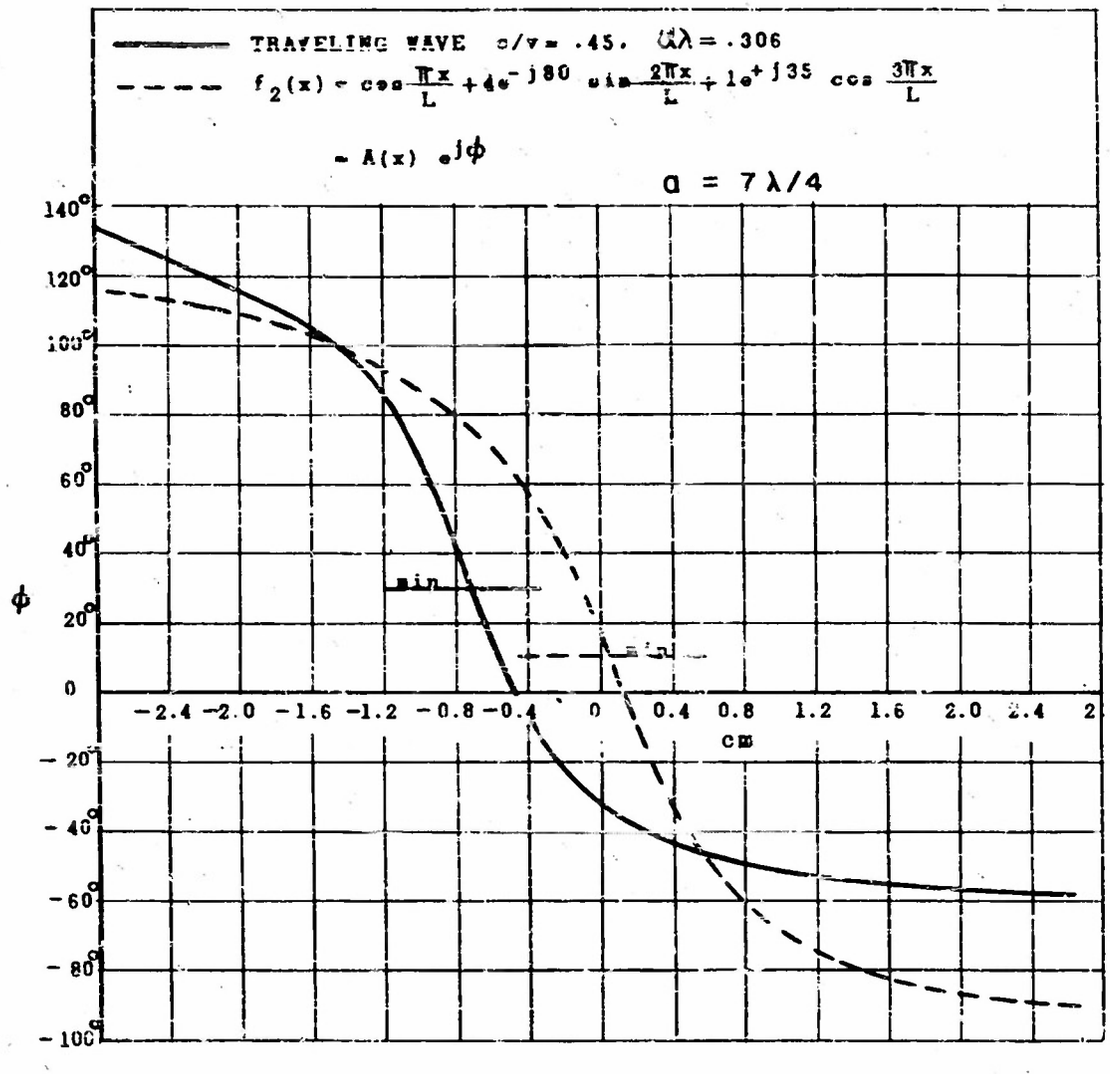

E_y APERTURE PHASE DISTRIBUTION

Graph 15

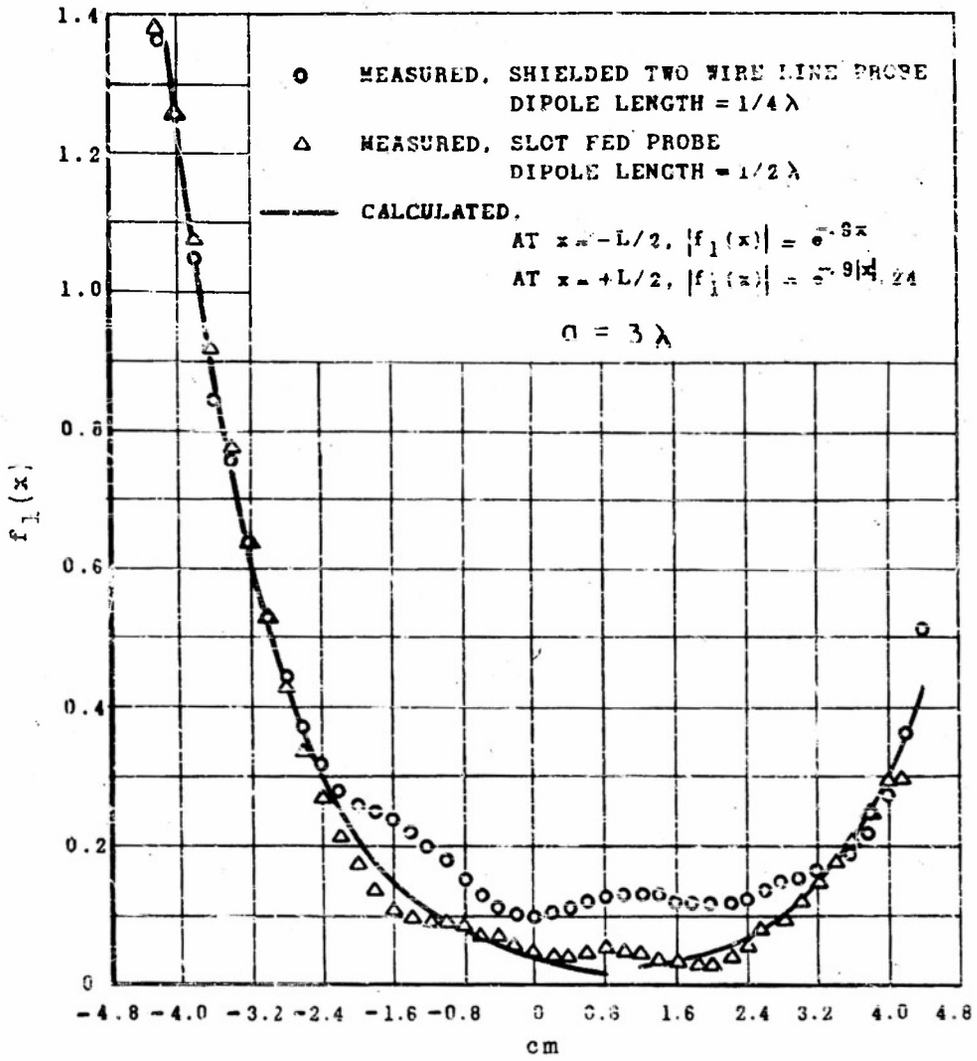

E_x APERTURE AMPLITUDE DISTRIBUTION

Graph 16

APPENDIX

I. Traveling Wave Integral

Given $f_2(x) = e^{-\gamma x} + \Gamma e^{-2\gamma a} e^{\gamma x}$

where Γ = reflection coefficient of slot edge = -1

$\gamma = \alpha + jpk$

α = attenuation constant

$p = c/v$ = ratio of free space to traveling wave phase velocities

$k = 2\pi/\lambda$ = free space phase constant

Then for a slot of length $a = n\lambda/2$

$$\frac{1}{\lambda}\int_0^a f_2(x)\, e^{jkKx}\, dx = \left(\frac{1 - e^{-n\pi(p-K)}\, e^{-n/2\alpha\lambda}}{\alpha\lambda + j\,2\pi(p-K)}\right) + \Gamma e^{-n/2\alpha\lambda}\, e^{-jn\pi(p-K)}\left(\frac{1 - e^{-n/2\alpha\lambda}\, e^{-jn\pi(p+K)}}{\alpha\lambda + j2\pi(p+K)}\right) \quad (13)$$

To obtain $E_y(\psi)$ by equation (10) of section II

set $K = \sin\alpha \sin\psi$

For all measurements of $E_y(\psi)$, the receiving horn is positioned at $\sin\alpha = .875$. Simplification of equation (13) is unnecessary since it is the most convient form for graphical computation.

II. Standing Wave Integrals

For a slot of length $a = n\lambda/2$, supporting the m^{th} cosine or sine mode:

$$\frac{\pi}{\lambda}\int_{-\frac{a}{2}}^{+\frac{a}{2}} \cos\left(\frac{m\pi x}{a}\right) e^{jkKx}\, dx = \frac{-K}{\left[\left(\frac{m}{n}\right)^2 - K^2\right]} \cos\left(\frac{m\pi}{2}\right)\sin\left(\frac{Kn\pi}{2}\right) + \frac{m}{n}\,\frac{\sin\left(\frac{m\pi}{2}\right)\cos\left(\frac{Kn\pi}{2}\right)}{\left[\left(\frac{m}{n}\right)^2 - K^2\right]} \quad (14)$$

$$\frac{1}{\lambda}\int_{-\frac{a}{2}}^{+\frac{a}{2}} \sin\left(\frac{m\pi x}{a}\right) e^{jkKx}\,dx = \frac{jK \sin\left(\frac{m\pi}{2}\right)\cos\left(\frac{Kn\pi}{2}\right)}{\left[\left(\frac{m}{n}\right)^2 - K^2\right]} - \frac{j\frac{m}{n}\cos\left(\frac{m\pi}{2}\right)\sin\left(\frac{Kn\pi}{2}\right)}{\left[\left(\frac{m}{n}\right)^2 - K^2\right]} \qquad (15)$$

where $K = \sin\theta$ for patterns in the planes $\phi = 0^\circ$ and $\phi = 90^\circ$.

III. Interference Pattern from Slot Edge Sources

The slot extends from $x = 0$ to $x = a = n\lambda/2$. The sources have E_x polarization and have the following step form:

$$E_x(x) = 1 \quad \text{for} \quad \lambda/8 \geq x \geq 0$$

$$E_x(x) = 0 \quad \text{for} \quad a - \lambda/8 > x > \lambda/8$$

$$E_x(x) = A\,e^{j\delta} \quad \text{for} \quad a \geq x \geq a - \lambda/8$$

where A is a real constant

δ is a constant phase angle

Then, in the plane $\phi = 0^\circ$, and for $E_x(y) = \cos\frac{\pi y}{b}$, equation (5) in section II gives

$$E_\theta(\theta) = \frac{j}{32R}\,e^{-jkR}\,\frac{\sin\frac{\pi K}{8}}{\frac{\pi K}{8}}\,e^{j\frac{\pi K}{8}}\left(1 + Ae^{j\delta}e^{j2K\pi\left[\frac{n}{2}-\frac{1}{8}\right]}\right) \qquad (16)$$

where $K = \sin\theta$

For the specific case of $a = n\lambda/2 = 3\lambda$ ($n = 6$), the relative phase angle δ was obtained from the first positive maxima in figure (10) by the equation:

$$\delta + 2\pi \sin\theta\left(\frac{n}{2} - \frac{1}{8}\right) = 0 \qquad (17)$$

where $\theta = 6.9^\circ$.

By (17) δ is found $= -124^\circ$. A is arbitrarily chosen equal to .4 giving coincidence with the measured maximum and minimum at, respectively, $\theta = -13^\circ$ and $\theta = -23.5^\circ$.

REFERENCES

1. Watson, W. H., "The Physical Principles of Wave Guide Transmission and Antenna Systems", Oxford, The Clarendon.

2. Silver, S., Editor, "Microwave Antenna Theory and Design", M.I.T. Radiation Laboratory Series, vol. 12, McGraw Hill Company, 1949.

3. Booker, H. G., "Slot Aerials and their Relation to Complementary Wire Aerials", J.I.E.E., vol. 93, Pt. IIIA, No. 4, PP. 620-676, (1946).

4. Ohio State Research Foundation, "Flush Mounted Antennas", Columbus, Ohio, (Report period, Sept. 6 to Dec. 5, 1950).

5. de Andrade, P.E., "Rectangular Apertures in Circular Waveguides", Report No. 183, Antenna Laboratory, University of California, 1951.

6. Friedigkeit, J. H., "The Use of Resistance Material for Absorbing Microwave Radiation", Antenna Laboratory, Report No. 183, University of California, 1950.

Distribution List

Chief of Naval Research, Washington, D. C. (Code 427).....2
Naval Research Laboratory, (Code 2000).....6
Chief of Naval Research, (Code 460).....1
Naval research Laboratory (Code 2021).....2
Naval Research Laboratory (Code 3180).....1
BuShips (Code 3[illegible]).....1
BuShips (Code 838).....1
Bureau of Ordnance (Re4f).....1
Bureau of Ordnance (ND3).....1
Bureau of Aeronautics (EL51).....1
Bureau of Aeronautics (EL1).....1
Chief of Naval Operations (Op-413).....1
Chief of Naval Operations (Op-20).....1
Chief of Naval Operations (Op-32).....1
Naval Air Development Station, Electronics Laboratory.....1
O.N.R., New York.....1
O.N.R., San Francisco.....2
O.N.R., Chicago, Illinois.....1
O.N.R., Pasadena, California.....1
O.N.R., Fleet Post Office.....2
Naval Ordnance Laboratory.....1
U.S.N.E.L., San Diego, California.....2
U.S. Naval Academy, Electrical Eng. Dept., Monterey.....1
Commandant Coast Guard (EEE).....1
Office of the Chief Signal Officer (SIGET).....1
Signal Corps Engineering Laboratories, Attn: Mr. Woodyard.....1
Electronics Laboratory, Wright Field (MCREER).....1
AMC Watson Laboratories, Attn: Dr. P. Newman.....1
AMC Cambridge Research Laboratory, Attn: Dr. Spencer.....1
Headquarters, U.S. Air Force (AFDEN-2).....1
Research and Development Board, Washington, D.C.....1
National Bureau of Standards.....1
Cruft Laboratory, Harvard University, Attn: Prof. King.....1
Mass. Institute of Technology, Attn: Prof. L. J. Chu.....1
Stanford University, Attn: Dean F. E. Terman.....1
E.E. Department, Illinois University, Attn: Prof. Jordan.....1
Ohio State University Research Foundation, Dr. Rumsey.....1
E.E. Department, Cornell University, Attn: Dr. H. G. Booker.....1
Stanford Research Institute, Attn: Dr. J.V.N. Granger.....1
Polytechnic Institute of Brooklyn, Attn: Dr. A. Oliner.....1
Washington Square College, N.Y.U. Math Group, Attn: Prof. Kline.....1
Squier Signal Laboratory, Attn: Vincent J. Rublin.....1
Flight Determination Laboratory, Attn: M.A. Krivanich.....1
Department of Commerce.....1
Armed Services Technical Information Agency.....5